

UNCLASSIFIED

AD NUMBER

ADB018629

LIMITATION CHANGES

TO:

Approved for public release; distribution is unlimited.

FROM:

Distribution authorized to U.S. Gov't. agencies only; Test and Evaluation; MAY 1977. Other requests shall be referred to Space and Missile Systems Organization, Attn:SKF, P. O. Box 92960, Worldway Postal Center, Los Angeles, CA 90009.

AUTHORITY

USSD ltr, 9 May 1980

THIS PAGE IS UNCLASSIFIED



**QUALIFICATION TEST OF THE THIOKOL TE-M-364-19
SOLID-PROPELLANT ROCKET MOTOR
(S/N 19006)**

**ENGINE TEST FACILITY
ARNOLD ENGINEERING DEVELOPMENT CENTER
AIR FORCE SYSTEMS COMMAND
ARNOLD AIR FORCE STATION, TENNESSEE 37389**

May 1977

Final Report for Period — February 4, 1977

Distribution limited to U.S. Government agencies only; this report contains information on test and evaluation of military hardware; May 1977; other requests for this document must be referred to Space and Missile Systems Organization (SKF), PO Box 92960, Worldway Postal Center, Los Angeles, California 90009.

Prepared for

**SPACE AND MISSILE SYSTEMS ORGANIZATION (SKF)
PO BOX 92960, WORLDWAY POSTAL CENTER
LOS ANGELES, CALIFORNIA 90009**

NOTICES

When U. S. Government drawings specifications, or other data are used for any purpose other than a definitely related Government procurement operation, the Government thereby incurs no responsibility nor any obligation whatsoever, and the fact that the Government may have formulated, furnished, or in any way supplied the said drawings, specifications, or other data, is not to be regarded by implication or otherwise, or in any manner licensing the holder or any other person or corporation, or conveying any rights or permission to manufacture, use, or sell any patented invention that may in any way be related thereto.

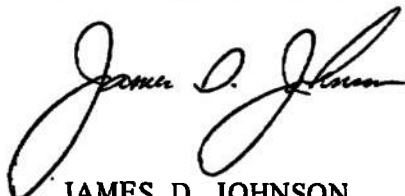
Qualified users may obtain copies of this report from the Defense Documentation Center.

References to named commercial products in this report are not to be considered in any sense as an endorsement of the product by the United States Air Force or the Government.

APPROVAL STATEMENT

This technical report has been reviewed and is approved for publication.

FOR THE COMMANDER



JAMES D. JOHNSON
Lt Colonel, USAF
Chief Air Force Test Director, ETF
Directorate of Test



ALAN L. DEVEREAUX
Colonel, USAF
Director of Test

UNCLASSIFIED

REPORT DOCUMENTATION PAGE		READ INSTRUCTIONS BEFORE COMPLETING FORM
1 REPORT NUMBER AEDC-TR-77-59	2 GOVT ACCESSION NO	3 RECIPIENT'S CATALOG NUMBER
4 TITLE (and Subtitle) QUALIFICATION TEST OF THE THIOKOL TE-M-364-19 SOLID-PROPELLANT ROCKET MOTOR (S/N 19006)	5 TYPE OF REPORT & PERIOD COVERED Final Report - February 4, 1977	
	6 PERFORMING ORG REPORT NUMBER	
7 AUTHOR(s) H. L. Merryman - ARO, Inc.	8 CONTRACT OR GRANT NUMBER(s)	
9 PERFORMING ORGANIZATION NAME AND ADDRESS Arnold Engineering Development Center (XO) Air Force Systems Command Arnold Air Force Station, Tennessee 37389	10 PROGRAM ELEMENT, PROJECT, TASK AREA & WORK UNIT NUMBERS Program Element 920B09	
11 CONTROLLING OFFICE NAME AND ADDRESS Space and Missile Systems Organization (SKF), P. O. Box 92960, Worldway Postal Center, Los Angeles, California 90009	12 REPORT DATE May 1977	
	13 NUMBER OF PAGES 60	
14 MONITORING AGENCY NAME & ADDRESS (if different from Controlling Office)	15. SECURITY CLASS. (of this report) UNCLASSIFIED	
	15a DECLASSIFICATION DOWNGRADING SCHEDULE N/A	
16 DISTRIBUTION STATEMENT (of this Report) Distribution limited to U. S. Government agencies only; this report contains information on test and evaluation of military hardware; May 1977; other requests for this document must be referred to Space and Missile Systems Organization (SKF), P. O. Box 92960, Worldway Postal Center, Los Angeles, California 90009.		
17 DISTRIBUTION STATEMENT (of the abstract entered in Block 20, if different from Report)		
18 SUPPLEMENTARY NOTES Available in DDC		
19 KEY WORDS (Continue on reverse side if necessary and identify by block number) solid-propellant rocket motor ballistics altitude simulation structural stability TE-M-364-19 spin stabilization performance		
20 ABSTRACT (Continue on reverse side if necessary and identify by block number) One Thiokol Chemical Corporation TE-M-364-19 solid-propellant rocket motor was fired while spinning at 60 rpm about its axial centerline. The motor was ignited at a simulated altitude of 122,000 ft, following temperature conditioning at 15 ± 5°F for a minimum of 44 hr. The program objectives of determining vacuum ballistic performance, altitude ignition characteristics, motor		

UNCLASSIFIED

UNCLASSIFIED

20. ABSTRACT (Continued)

temperature-time history, the lateral (nonaxial) thrust vector, and structural integrity of the motor components are presented and discussed.

UNCLASSIFIED

PREFACE

The work reported herein was conducted at the Arnold Engineering Development Center (AEDC), Air Force Systems Command (AFSC), at the request of the Space and Missile Systems Organization (SAMSO), AFSC, for TRW, Inc., Redondo Beach, California, under Program Element 920B09. The results of the test were obtained by ARO, Inc., AEDC Division (a Sverdrup Corporation Company), operating contractor for the AEDC, AFSC, Arnold Air Force Station, Tennessee, under ARO Project Number R41C-37A. The author of this report was H. L. Merryman, ARO, Inc. The data analysis was completed on April 11, 1977, and the manuscript (ARO Control No. ARO-ETF-TR-77-29) was submitted for publication on April 14, 1977.

CONTENTS

	<u>Page</u>
1.0 INTRODUCTION	5
2.0 APPARATUS	5
3.0 PROCEDURES	8
4.0 RESULTS AND DISCUSSION	10
5.0 SUMMARY OF RESULTS	12
REFERENCES	14

ILLUSTRATIONS

Figure

1. Thiokol Chemical Corporation TE-M-364-19 Solid-Propellant Rocket Motor	15
2. Installation of the Thiokol TE-M-364-19 Rocket Motor in Propulsion Development Test Cell (T-3)	17
3. Instrumentation Locations	20
4. Variation of Thrust and Chamber Pressure during Motor Ignition	22
5. Variation of Thrust and Chamber Pressure during Firing	23
6. Comparison of Exhaust Ducting Pressures during Firing	24
7. Postfire Photograph of Motor Assembly	25
8. Motor Temperature Variation with Time	27
9. Variation of Lateral (Nonaxial) Thrust Vector during Firing	45
10. Variation of Motor Case Strain during Firing	46
11. Variation of Nozzle Adapter Flange Strain during Firing	48

TABLES

1. Instrumentation Summary and Measurement Uncertainty	56
2. Summary of TE-M-364-19 Motor Performance	58
3. Summary of TE-M-364-19 Motor Physical Dimensions	59
4. Comparison of Development and Qualification Motor Tests	60

1.0 INTRODUCTION

The Thiokol Chemical Corporation (TCC) TE-M-364-19 solid-propellant rocket motor is to be used as the apogee kick motor in the Fleet Satellite Communications System (FLTSATCOM). The kick motor is designed to impart the required impulse to inject the FLTSATCOM satellite into a geostationary orbit from a transfer orbit (Ref. 1).

The test program reported herein was a portion of the qualification testing program for the TE-M-364-19 motor. Testing of two development motors was conducted in 1973 (Ref. 2), and one qualification motor in 1974 (Ref. 3). The test objectives were to determine the vacuum ballistic performance, altitude ignition characteristics, motor component structural integrity, motor temperature time history, and the lateral (nonaxial) thrust component. The motor was fired while spinning about its axial centerline at 60 rpm following temperature conditioning at $15 \pm 5^\circ\text{F}$ for a minimum of 44 hr.

Motor ballistic performance, altitude ignition characteristics, motor temperature time history, motor component structural integrity, and the lateral (nonaxial) thrust data are presented and, where applicable, compared with the requirements outlined in Refs. 1 and 4.

2.0 APPARATUS

2.1 TEST ARTICLE

The Thiokol Chemical Corporation TE-M-364-19 solid-propellant rocket motor (Fig. 1) is a full-scale, flightweight motor having the following nominal dimensions:

Motor OD	38 in.
Overall Length	60 in.
Loaded Weight	2,060 lbm
Propellant Weight	1,900 lbm
ICC Classification	2
Nozzle Throat Area	10.9 in. ²
Nozzle Expansion Ratio	40.9:1

The elongated spherical motor case is constructed of 6Al-4V titanium alloy with a wall thickness of 0.052 in. in the hemispherical end sections and 0.093 in. in the cylindrical center section. The base is lined internally with TCC TL-H-304 liner and insulated with TIR-300 asbestos-polyisoprene. The nozzle assembly contains a Graph-I-Tite® G-90 graphite

throat insert. The exit cone is constructed of tape-wrapped carbon phenolic. The nozzle assembly has a nominal 40.9:1 expansion ratio and a 14.2-deg half-angle at the exit plane. The nozzle plug, a conical foam closure (Fig. 1a), was removed from the nozzle throat prior to firing.

The TE-M-364-19 rocket motor contains a composite propellant grain formulation designated TP-H-3062 (ICC Class 2) cast in an eight-point-star configuration. This motor contained approximately 40 lbm more propellant than the previous motors (Refs. 2 and 3).

Ignition was accomplished by one pyrogen igniter, which, in the flight configuration, incorporates two initiators, and a single electromechanical safe-and-arm (S/A) device. For the tests reported herein, one initiator was used. The pyrogen assembly contained a 19-gm BKNO_3 charge that ignited the TP-H-3062 pyrogen cartridge.

2.2 INSTALLATION

The motor assembly was installed in Propulsion Development Test Cell (T-3) (Fig. 2) inside a cryoplate assembly through which cooled trichloroethylene was circulated to provide the conditioning temperature. The motor assembly was cantilever mounted from the spindle face of the spin fixture assembly. The spin assembly was mounted on a thrust cradle, which was supported from the cradle support stand by three vertical and two horizontal double-flexure columns (Fig. 2c). The spin fixture assembly consists of a 10-hp squirrel-cage-type drive motor, a thrust bearing assembly, and a 46-in.-long spindle having a 36-in.-diam aft spindle face. The spin fixture rotated counterclockwise, looking upstream. Electrical leads to and from the igniters, pressure transducers, strain grids, and thermocouples on the rotating motor were provided through a 170-channel slipring assembly mounted between the forward and aft bearing assemblies of the spindle. Axial thrust was transmitted through the spindle-thrust bearing assembly to two double-bridge strain-gage-load cells mounted just forward of the thrust bearing on the motor axial centerline.

Preignition pressure altitude conditions were maintained in the test cell by a steam ejector operating in series with the ETF exhaust gas compressors. During the motor firing, the motor exhaust gases were used as a driving gas for the 42-in.-diam, water-cooled, ejector-diffuser system incorporating a 24-deg (half-angle) conical inlet to maintain test cell pressure at an acceptable level. There was a 3.0-in. gap between the nozzle exit plane and the entrance of the diffuser; the conical section intersected the cylindrical portion of the diffuser 8.0 in. from the entrance.

2.3 INSTRUMENTATION

Instrumentation was provided to measure axial force, motor chamber pressure (through the pyrogen), lateral (nonaxial) force, test cell pressure, motorcase and nozzle temperatures, motor case and nozzle strains, and motor rotational speed. Table 1 presents instrument ranges, recording methods, and measurement uncertainty for all reported parameters.

The axial force measuring system consisted of two double-bridge, strain-gage-type load cells mounted in the axial double-flexure column forward of the thrust bearing on the spacecraft centerline. The lateral (nonaxial) force measuring system consisted of two double-bridge, strain-gage-type load cells installed forward and aft between the flexure-mounted cradle support stand normal to the rocket motor axial centerline in the horizontal plane passing through the motor axial centerline (Fig. 2c).

Unbonded strain-gage-type transducers (0 to 1 psia) were used to measure test cell pressure. Bonded strain-gage-type transducers with ranges from 0 to 15, 0 to 100, and 0 to 1,000 psia were used to measure motor chamber pressure through the pyrogen. Chromel®-Alumel® (CA) thermocouples were bonded to the motor case and nozzle (Fig. 3a) to measure surface temperatures during and after motor burn time. Rotational speed of the motor assembly was determined from the output of a magnetic pickup. Strain gages were bonded to the case and nozzle to measure longitudinal and hoop strains during the firing (Fig. 3b).

The output signal of each measuring device was recorded on independent instrumentation channels. Primary data were obtained from four axial thrust channels, three test cell pressure channels, and four motor chamber pressure channels. These data were recorded as follows: Each instrument output signal was recorded on magnetic tapes from a multi-input, analog-to-digital converter for reduction at a later time by an electronic digital computer. The thrust, chamber pressure, and test cell data channels were recorded at 1,000 samples per second. The thermocouples and strain grids were recorded at 100 samples per second.

The output signal from the magnetic rotational speed pickup was recorded in the following manner: A frequency-to-analog converter was triggered by the pulse output from the magnetic pickup and in turn supplied a square wave of constant amplitude to the electronic counter, magnetic tape, and oscillograph recorders. The scan sequence of the electronic counter was adjusted to directly display the motor spin rate in revolutions per minute.

The millivolt outputs of the lateral (nonaxial) force load cells were recorded on magnetic tape from a multi-input, analog-to-digital converter at a sampling rate of 1,000 samples per second and reduced to engineering units by an electronic computer.

Selected channels of thrust and pressures were recorded on null-balance, potentiometer-type strip charts for analysis immediately after a motor firing. Visual observation of the firing was provided by a closed-circuit television monitor. High-speed, motion-picture cameras provided a permanent visual record of the firings.

2.4 CALIBRATION

The thrust system calibrator weights, thrust load cells, and pressure transducers were laboratory calibrated prior to usage in this test. After installation of the measuring devices in the test cell, all systems were in-place calibrated at sea-level, nonspin, ambient conditions. The axial-force system was then deadweight calibrated at simulated altitude with the motor spinning at 60 rpm.

The pressure recording systems were calibrated by an electrical, four-step calibration using resistances in the transducer circuits to simulate selected pressure levels. The axial-thrust instrumentation systems were calibrated by applying to the thrust cradle known forces, which were produced by deadweights acting through a bell crank. The calibrator is hydraulically actuated and remotely operated from the control room. Thermocouple and strain-gage recording instruments were calibrated by using millivolt levels to simulate thermocouple outputs.

After the motor firings, with the test cell still at simulated altitude pressure, the recording systems were recalibrated to determine any shift.

Calibrations of the lateral (nonaxial) force measuring system were conducted using the procedure outlined in Ref. 5.

3.0 PROCEDURE

The TC TE-M-364-19 rocket motor Q2 (S/N 19006) arrived at the AEDC on December 3, 1976. The motor was visually inspected for possible shipping damage and radiographically inspected for grain cracks, voids, or separations and found to meet criteria provided by the manufacturer.

After completion of the initial X-rays, the motor was temperature cycled at ambient pressure for four complete thermal cycles from 15 to 115°F (48 hr at each temperature level per cycle). The motor was again X-rayed, and no changes from initial X-rays could be found.

After completion of temperature cycling, motor Q2 was subjected to sinusoidal and random vibration testing at the von Kármán Facility, AEDC. The sinusoidal survey consisted of a uniform logarithmic sweep from 5 to 200 Hz at a nominal sweep rate of 2 octaves per minute with a 1/2-g (0-peak) input in both the lateral and longitudinal axes. Random vibration in each axis consisted of the following:

<u>Frequency Range, Hz</u>	<u>Level</u>
20 to 150	Increase 6 db/octave to 0.045 g ² /Hz
150 to 2,000	0.045 g ² /Hz 9.3 g rms overall

After completion of vibration conditioning, motor Q2 underwent radiographic inspection for the third time; no separations or discontinuities were found at any time during radiographic inspection, and no changes from initial X-rays could be found.

After the final radiographic inspection, motor Q2 was stored in an area temperature conditioned at $70 \pm 5^{\circ}\text{F}$ where the motor was checked to ensure correct fit of mating hardware, the electrical resistance of the igniter detonator device (initiator) was measured, the nozzle throat and exit diameters were measured, and the entire assembly was weighed and photographed. After the motor case was secured to the thrust adapter, the assembly was mounted on a spin table, and radial dimensions of selected surfaces were measured as a function of angular position relative to the entire centerline of the assembly to facilitate alignment with the spin-rig spin axis during test cell installation.

After installation of the motor assembly in the test cell, the motor centerline was axially aligned with the spin-rig spin axis by rotating the motor assembly and measuring the deflection of the selected surfaces with dial indicators and making appropriate adjustments. Instrumentation connections were completed, and the motor assembly was balanced at a rotational speed of 60 rpm.

Motor Q2 was installed in a cryoplate assembly (Fig. 2b), through which cooled trichloroethylene was circulated to provide the desired thermal environment of $15 \pm 5^{\circ}\text{F}$ for a minimum of 44 hr prior to motor firing. A dry gaseous-nitrogen purge was circulated within the space between the cryoplates and the motor case to remove water vapor which could condense as frost on the plate internal surfaces.

The final operation prior to firing was to adjust the firing circuit resistance to provide the desired current to the igniter detonator. The entire instrumentation measuring-recording complex was activated, and the motor was fired while spinning (under power) at 60 rpm.

Spinning was continued for approximately 60 min after burnout. During this time, postfire calibrations were accomplished, and motor temperatures were recorded continuously for 260 sec after ignition and then every 30 sec until 6 min after burnout. The assembly was decelerated slowly until rotation had stopped, and another set of calibrations was taken. The test cell pressure was then returned to ambient conditions, and the motor assembly was inspected, photographed, and removed to the storage area. Postfire inspection at the storage area consisted of measuring the exit diameter of the nozzle (the throat insert had fallen into the motor chamber after the firing, and the postfire throat diameter could not be obtained), weighing the motor, and photographically recording the postfire condition of the motor.

4.0 RESULTS AND DISCUSSION

One Thiokol Corporation TE-M-364-19 solid-propellant rocket motor (S/N 19006/Q2) was successfully fired at an ignition pressure altitude of 122,000 ft while spinning about its axial centerline at 60 rpm. Prior to firing, the motor was temperature conditioned at $15 \pm 5^\circ\text{F}$ for a period in excess of 44 hr.

The program objectives were to determine vacuum ballistic performance, altitude ignition characteristics, motor temperature-time history, structural integrity of motor components, and the lateral (nonaxial) thrust vector. The applicable data were used to demonstrate compliance of the motor with requirements set forth in Refs. 1 and 4.

Altitude ignition characteristics and vacuum ballistic performance are presented in Table 2. A temperature-time history of the motor case and nozzle is presented and discussed. When multiple channels of equal instrumentation were used to obtain values of a single parameter, the average values were used to calculate the data presented.

4.1 ALTITUDE IGNITION CHARACTERISTICS

Motor Q2 was ignited at a pressure altitude of 122,000 ft. The variation of thrust and chamber pressure during motor ignition are presented in Fig. 4. Chamber pressure was measured through the pyrogen port as it was during the previous firings (Refs. 2 and 3). Ignition delay time (t_d), the time interval from application of ignition voltage to the time that chamber pressure reaches 10 percent of maximum ignition pressure, was 0.004 sec, which was well below the specification maximum value of 0.500 sec. Ignition time (t_i), the time interval from application of ignition voltage to the time when chamber pressure has risen to 90 percent of the maximum chamber pressure reached during the first 500 msec, was 0.017 sec.

4.2 ALTITUDE BALLISTIC PERFORMANCE

The variations of thrust and chamber pressure with motor burn time are presented in Fig. 5. The maximum axial thrust value was 13,174 lbf, which was well below the specification maximum value of 15,000 lbf.

Action time, the time interval from the end of ignition time until chamber pressure reaches 100 psia on the descending portion of the pressure-versus-time curve, was 45.31 sec. There was no specification value for action time. Operation time, the time interval from the first perceptible indication of thrust until thrust returns to zero, was 53.93 sec; there was no specification value for operation time.

Immediately prior to firing, the solenoid valve to the cell pressure transducers was inadvertently closed voiding the test cell pressure measurement during the firing. Pressure measurements in the exhaust ducting downstream (Fig. 6) indicate that motor/diffuser operation during burning was equivalent to the previous motor test (Ref. 3). Therefore, for this test, the thrust vacuum correction ($P_a \times A_e$) was assumed to be equal to previous test (1,961 lbf-sec).

Vacuum total impulse based on operation time (t_{op}) was 545,152 lbf-sec and was well within the specification value of 545,999 lbf-sec \pm 1 percent. Vacuum specific impulse, based on the manufacturer's stated propellant weight and operation time (t_{op}), was 286.86 lbf-sec/lbm.

4.3 STRUCTURAL INTEGRITY AND TEMPERATURE DATA

Postfire examination of the motor case and nozzle assemblies did not reveal any evidence of thermal damage during the firing (Fig. 7). The pre- to postfire nozzle throat area increased 10.34 percent, and the nozzle exit area increased 1.20 percent (Table 3). The nozzle throat insert had fallen into the motor chamber after the firing, as was typical of tests of similar motors (Refs. 2 and 3). Thiokol Corporation supplied the postfire throat diameter.

Motor case and nozzle temperature variations with time are presented in Fig. 8. The maximum motor case temperature was about 465°F (T7B, Fig. 8f) and occurred about 200 sec after ignition. Maximum nozzle temperature was about 1,900°F (T15C, Fig. 8m) and occurred about 45 sec after ignition. The air temperature surrounding the nozzle (see Fig. 3a for thermocouple locations) reached about 2,105°F (T18A, Fig. 8r) and occurred about 46 sec after ignition.

4.4 LATERAL (NONAXIAL) THRUST VECTOR MEASUREMENT

A primary objective of this test was to measure the motor thrust misalignment. The objective was accomplished by measuring the lateral component of the axial thrust. The recorded lateral thrust data were corrected for installation and/or electronic effects as described in Ref. 5. The resultant data are presented in Fig. 9.

The maximum magnitude of lateral thrust recorded during the near steady-state portion of motor operation was about 7.0 lbf and occurred about 2 sec after motor ignition; average magnitude of lateral thrust measurement was about 4.5 lbf. The angular position corresponding to the maximum magnitude of lateral thrust was about 215 deg as measured clockwise looking upstream from the pyrogen pressure port.

4.5 MOTOR CASE AND NOZZLE ADAPTER FLANGE STRAIN

The two strain grids were bonded to the motor case. Figure 10 presents the variation of case strain with time. Maximum case strain was approximately 4,265 $\mu\text{in./in.}$ and occurred about 32 sec after ignition. Figure 11 presents the variation of nozzle adapter flange strain with time. Maximum strain in the nozzle was approximately 3,170 $\mu\text{in./in.}$ (tension) and occurred about 42 sec after ignition (Fig. 11).

4.6 COMPARISON WITH EARLIER MOTOR TESTS

Table 4 presents a comparison of the major performance data and physical dimensions of the two qualification and two development tests. The results from the tests indicated vacuum specific impulse, based on AEDC expanded mass, was an average of 285.1 lbf-sec/lbm for motors D1, Q1, and Q2, which were tested in the temperature range of 19 to 27°F. Motor D2 produced a vacuum specific impulse of 286.5 lbf-sec/lbm which was expected since it was tested at 111°F, about 90°F higher than the previously mentioned motors.

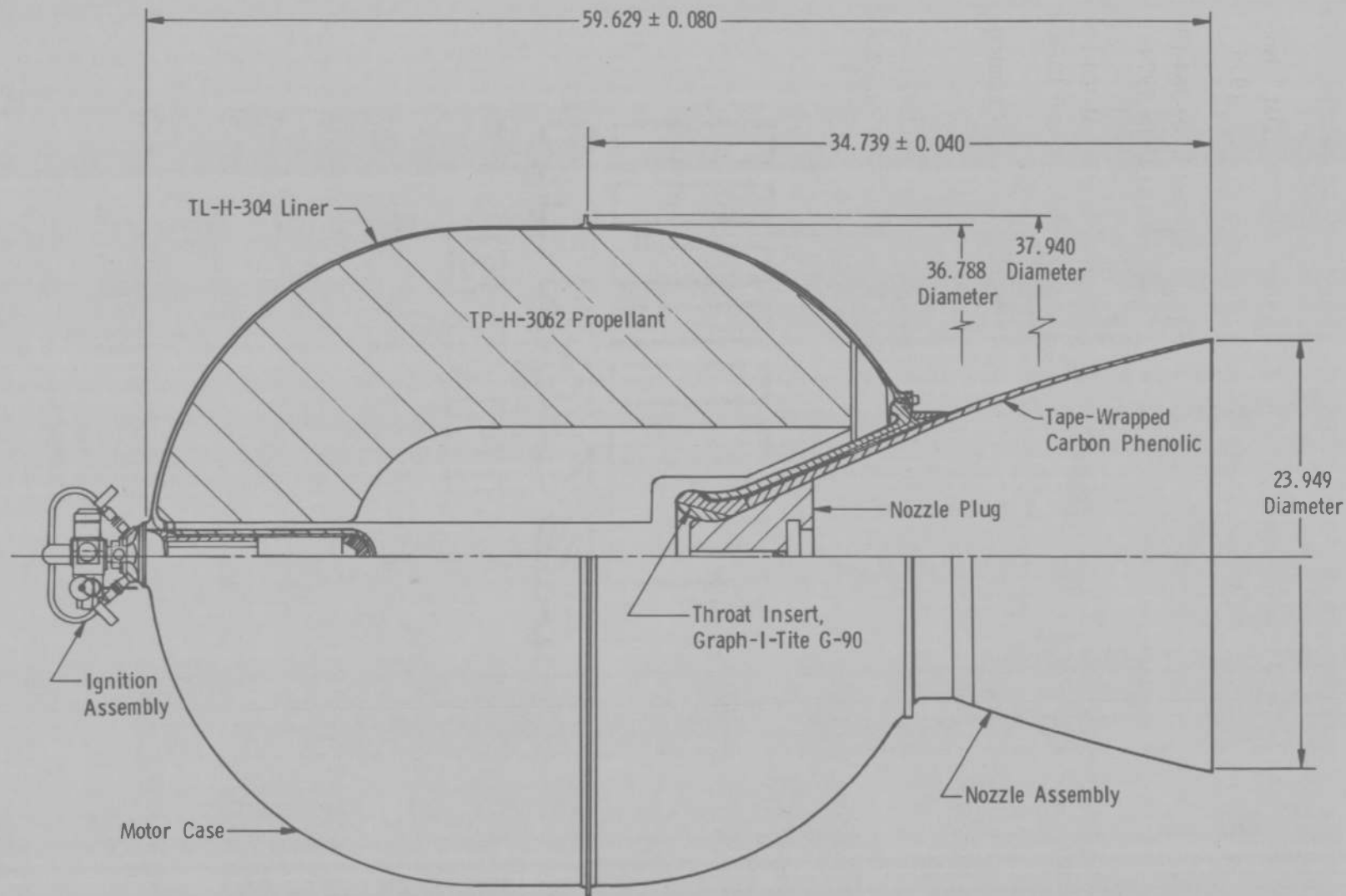
5.0 SUMMARY OF RESULTS

One Thiokol Corporation TE-M-364-19 solid-propellant rocket motor was fired while spinning about its axial centerline at 60 rpm. The motor was fired at an ignition pressure altitude of 122,000 ft following temperature conditioning at $15 \pm 5^\circ\text{F}$ for a minimum of 44 hr. The program objectives were to determine vacuum ballistic performance, altitude ignition characteristics, motor temperature time history, structural integrity of motor components, and the lateral (nonaxial) thrust vector. The applicable data were used to demonstrate compliance of the motor with requirements set forth in Ref. 1. The results are summarized as follows:

1. Ignition delay time, the time interval from the application of voltage to the time that chamber pressure reaches 10 percent of maximum ignition pressure, was 0.004 sec, which was well below the specification maximum value of 0.500 sec.
2. Ignition time, the time interval from application of ignition voltage to the time chamber pressure has risen to 90 percent of the maximum chamber pressure reached during the first 500 msec, was 0.017 sec. There was no specification value for ignition time.
3. Action time, the time interval from the end of ignition time until chamber pressure reaches 100 psia on the descending portion of the pressure-versus-time curve, was 45.31 sec. There was no specification value for action time.
4. Operation time, the time interval from the first perceptible indication of thrust until thrust returns to zero, was 53.93 sec; there was no specification value for operation time.
5. Vacuum impulse based on operation time was 545,152 lbf-sec and was within the specification value of 545,999 lbf-sec \pm 1 percent.
6. The maximum measured motor case temperature was about 465°F and occurred approximately 200 sec after ignition.
7. The maximum magnitude of lateral thrust recorded during the near steady-state portion of motor operation was about 7.0 lbf; the average magnitude of lateral thrust was about 4.5 lbf. The angular position corresponding to the maximum magnitude of lateral thrust was approximately 215 deg.
8. Maximum motor case strain was 4,265 μ in./in. and occurred about 32 sec after ignition.
9. Maximum strain in the nozzle was 3,170 μ in./in. and occurred about 42 sec after ignition.
10. Postfire examination of the motor case and nozzle assembly revealed no evidence of thermal damage during the firing.

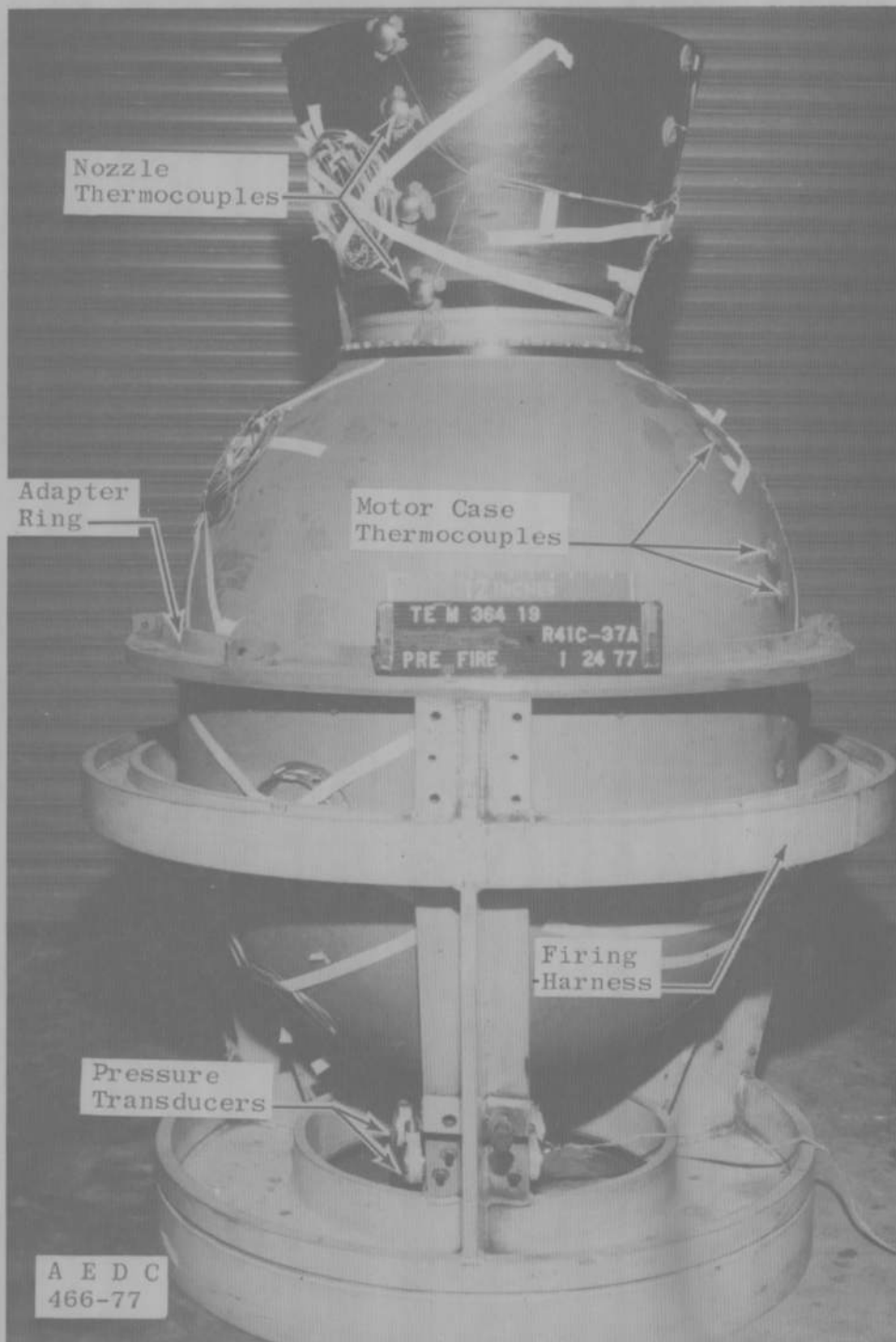
REFERENCES

1. Ellison, J. R. "Equipment Specification, Apogee Kick Motor, FLTSATCOM." No. Eq. 8-111, Rev. G. TRW, Redondo Beach, California, December 23, 1976.
2. Merryman, H. L. and Smith, L. R. "Development Test of the Thiokol TE-M-364-19 Solid-Propellant Rocket Motor." AEDC-TR-74-28 (AD919342L), May 1974.
3. Merryman, H. L. and Smith, L. R. "Qualification Test of the Thiokol TE-M-364-19 Solid-Propellant Rocket Motor." AEDC-TR-74-105 (AD923294L), October 1974.
4. Rowe, W. H. "Static Test for TE-M-364-19 Rocket Motor." Thiokol Chemical Corporation, Elkton, Maryland, November 22, 1976.
5. Nelius, M. A. and Harris, J. E. "Measurements of Nonaxial Forces Produced by Solid-Propellant Rocket Motors Using a Spin Technique." AEDC-TR-65-228 (AD474410), November 1965.

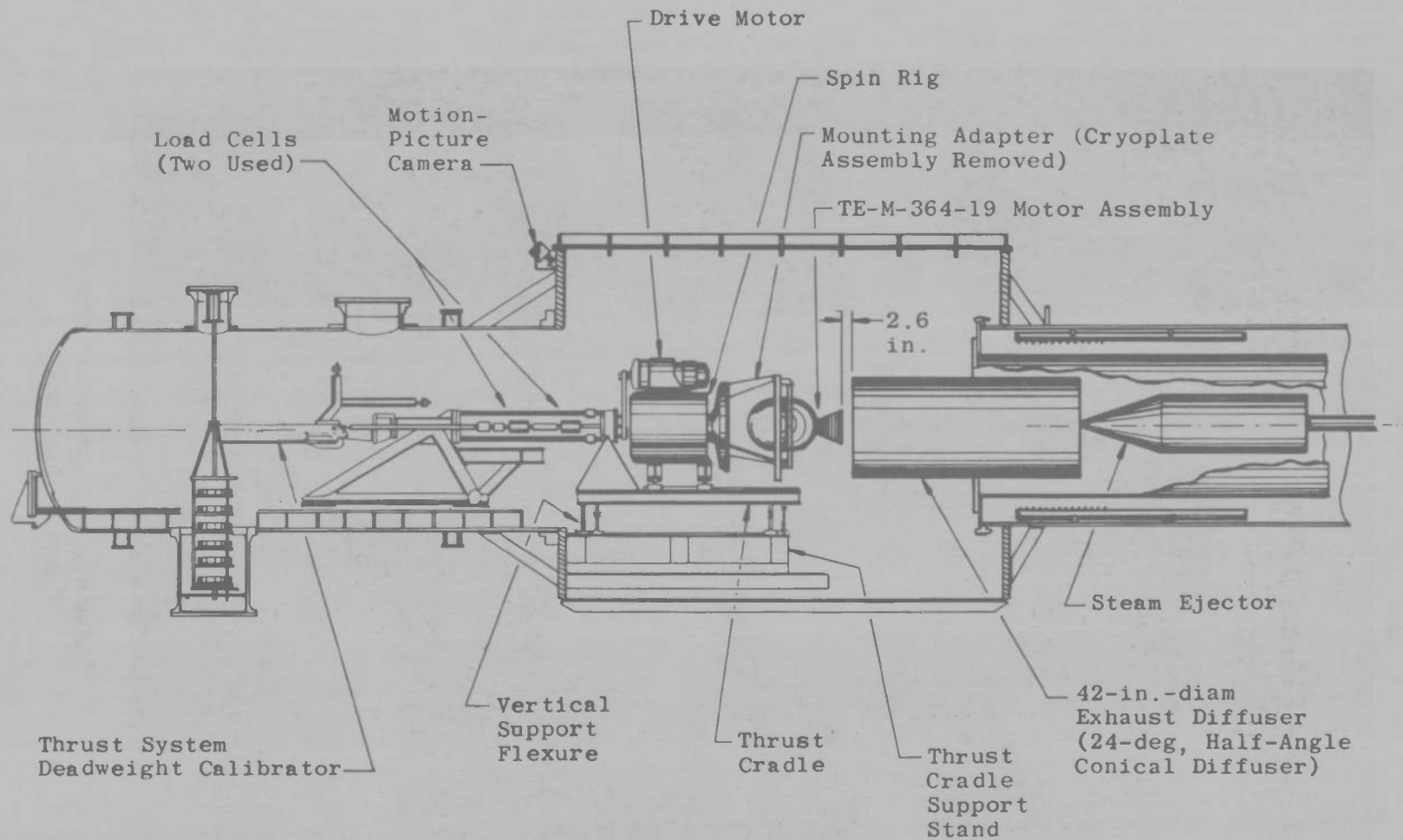


a. Schematic

Figure 1. Thiokol Chemical Corporation TE-M-364-19 solid-propellant rocket motor.

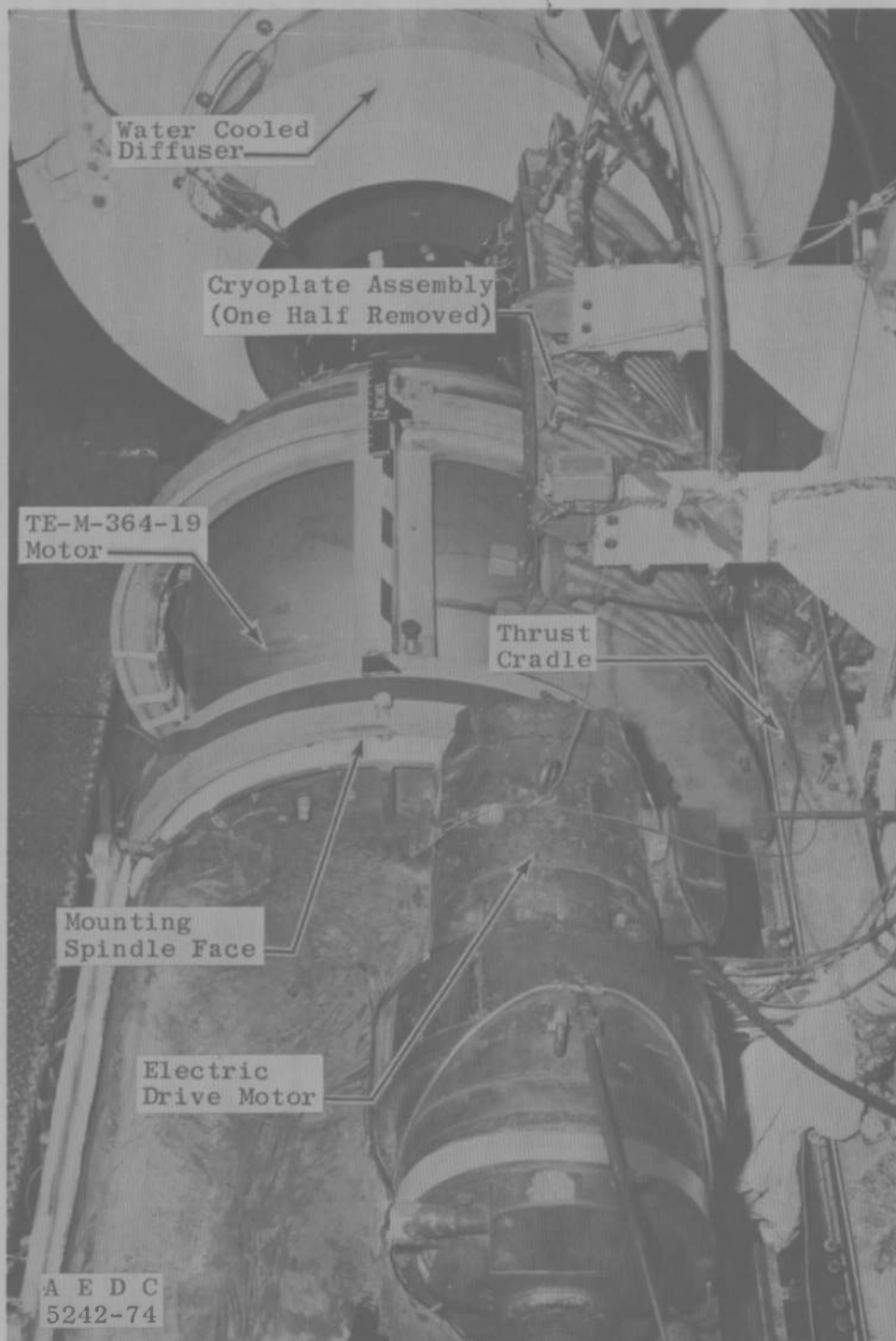


b. Photograph
Figure 1. Concluded.

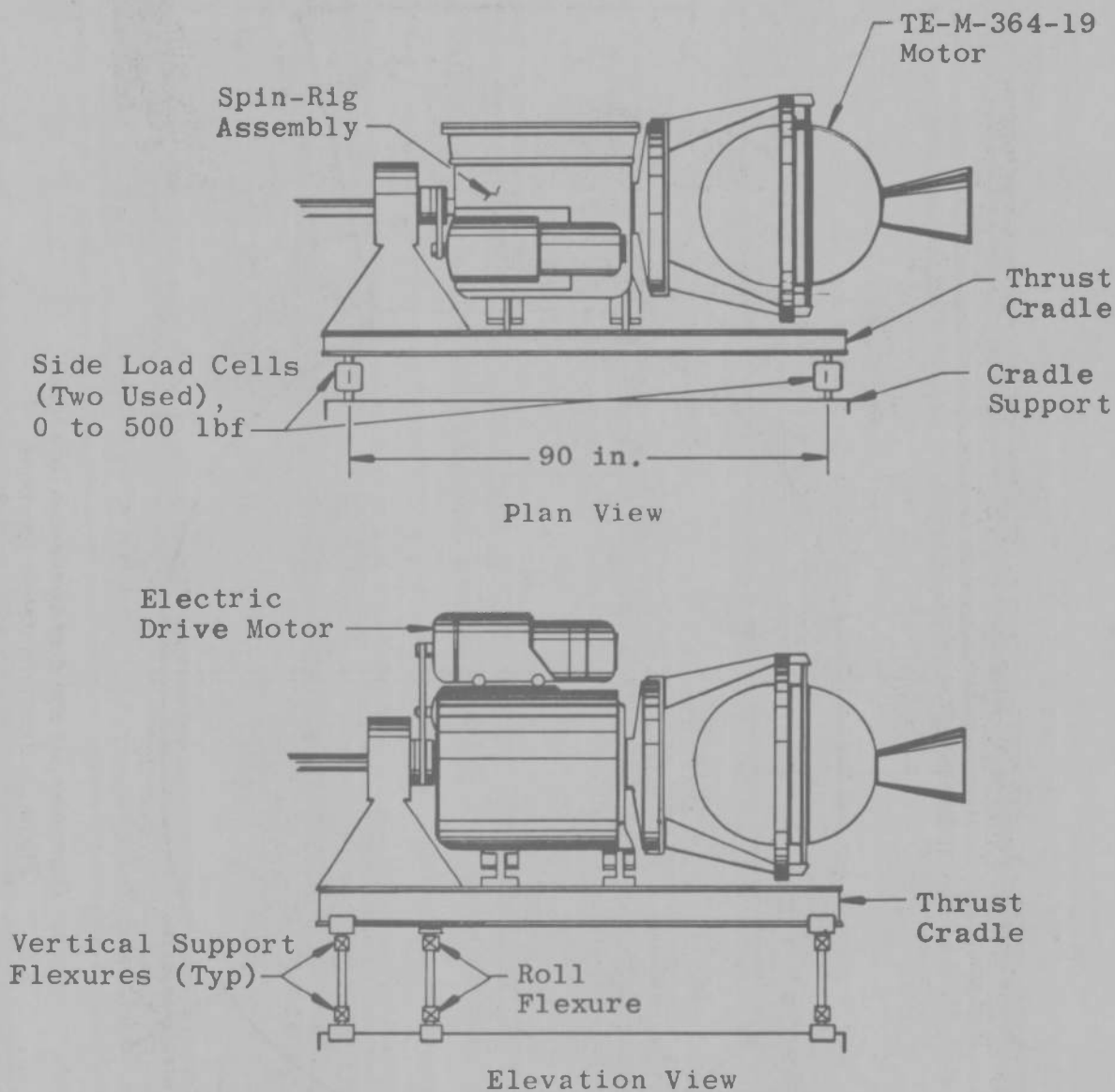


a. Schematic

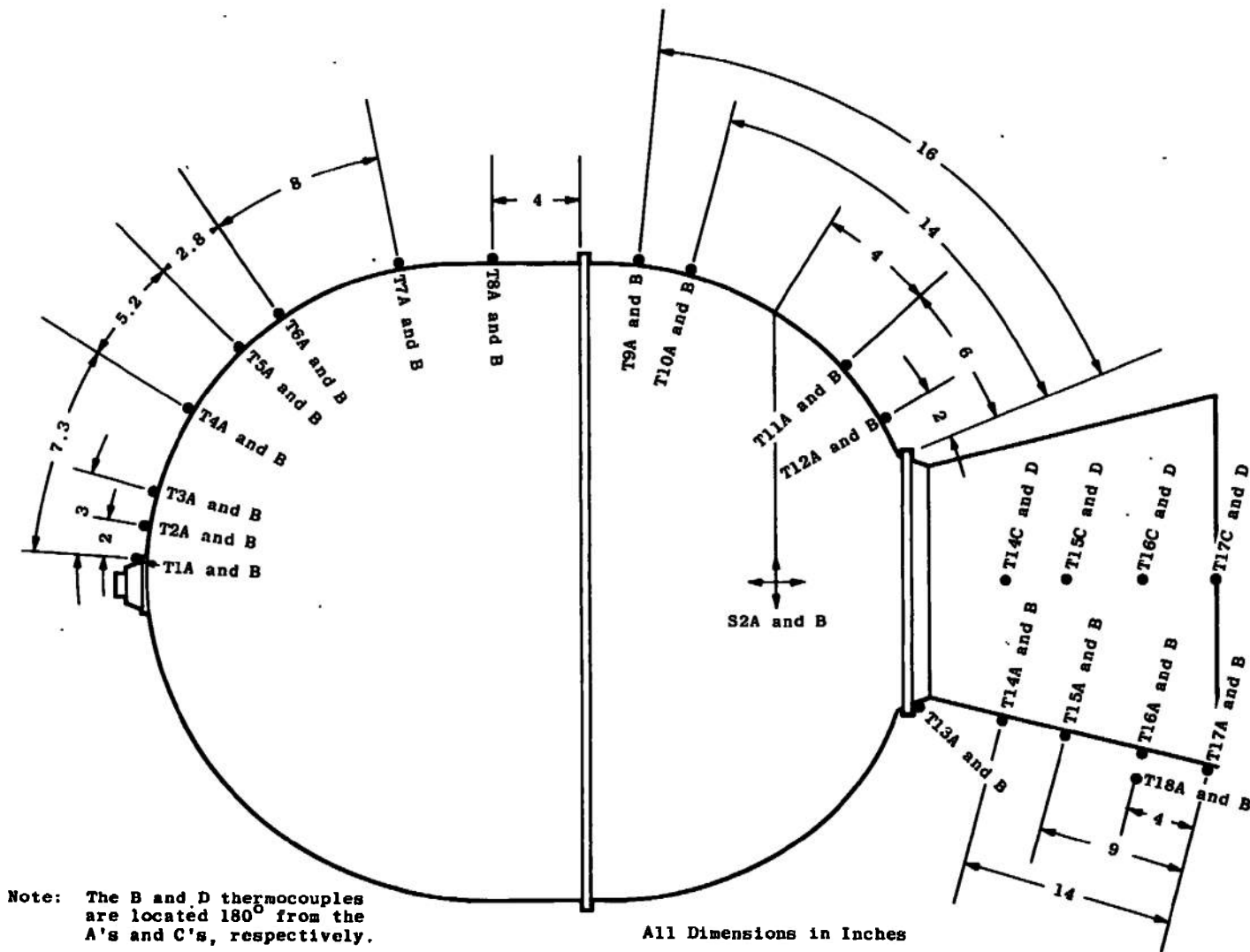
Figure 2. Installation of the Thiokol TE-M-364-19 rocket motor in Propulsion Development Test Cell (T-3).

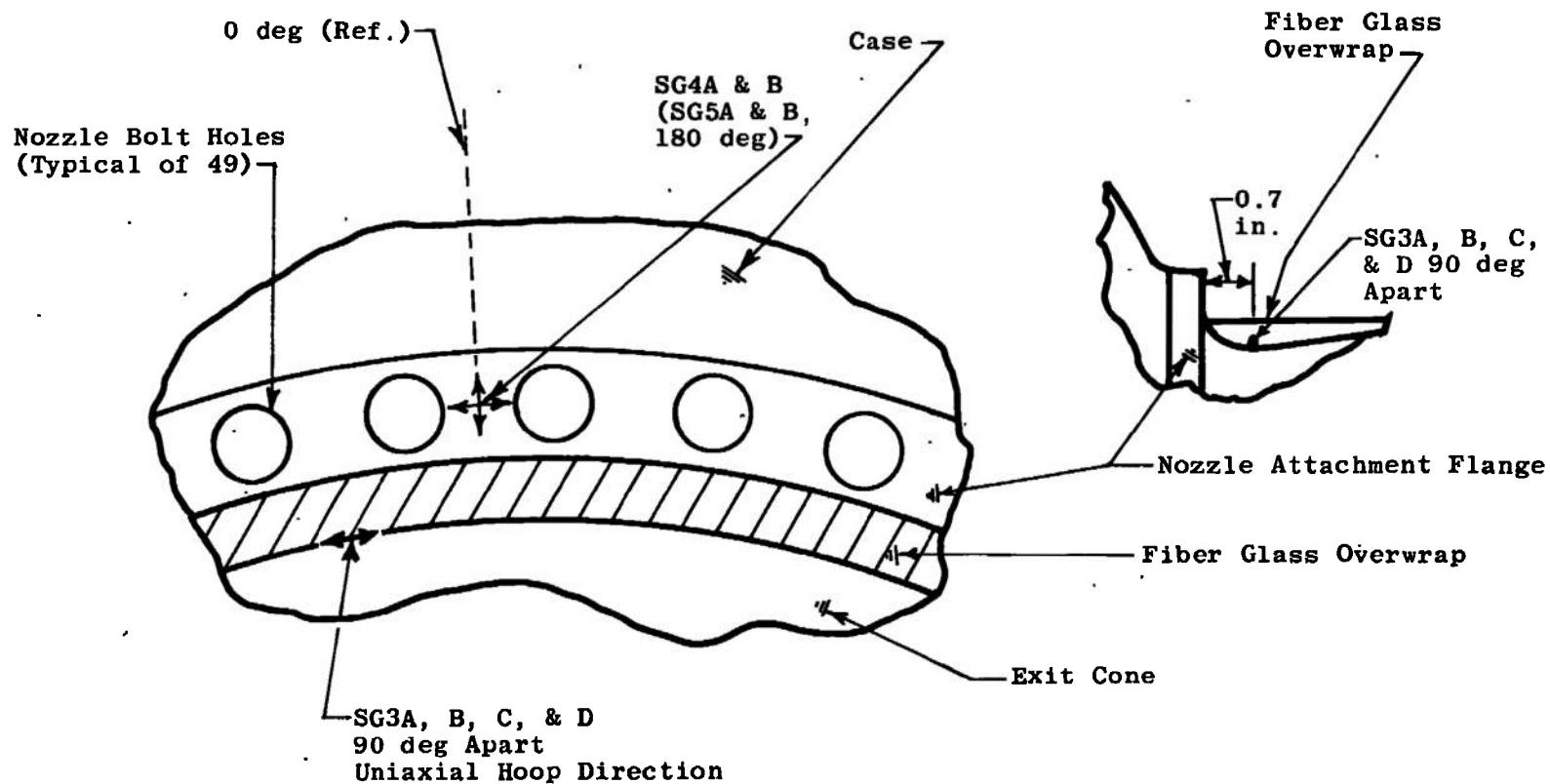


b. Photograph (view looking downstream)
Figure 2. Continued.



c. Detail of lateral (nonaxial) force measuring system
Figure 2. Concluded.





b. Nozzle strain-gage locations
Figure 3. Concluded.

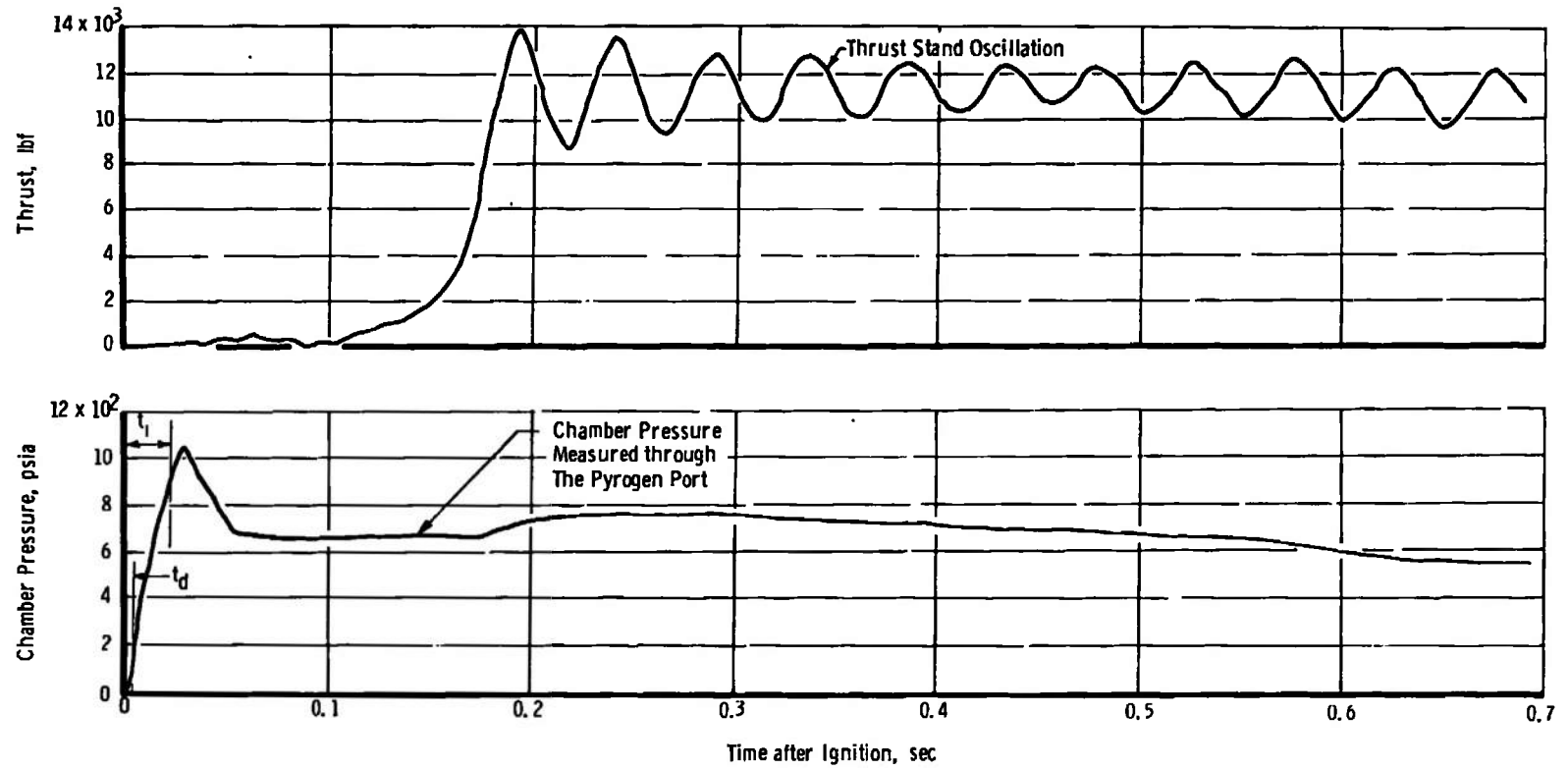


Figure 4. Variation of thrust and chamber pressure during motor ignition.

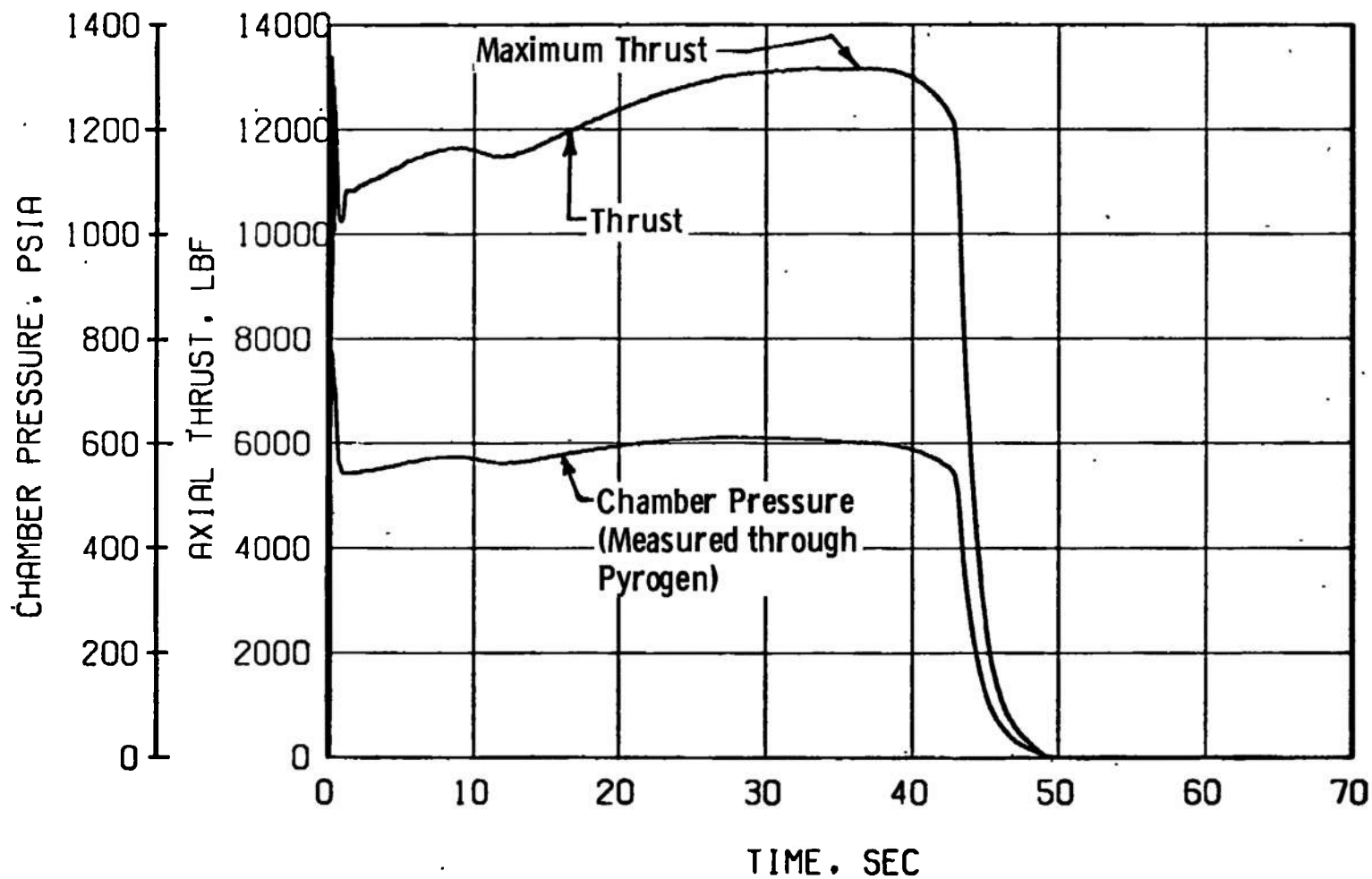


Figure 5. Variation of thrust and chamber pressure during firing.

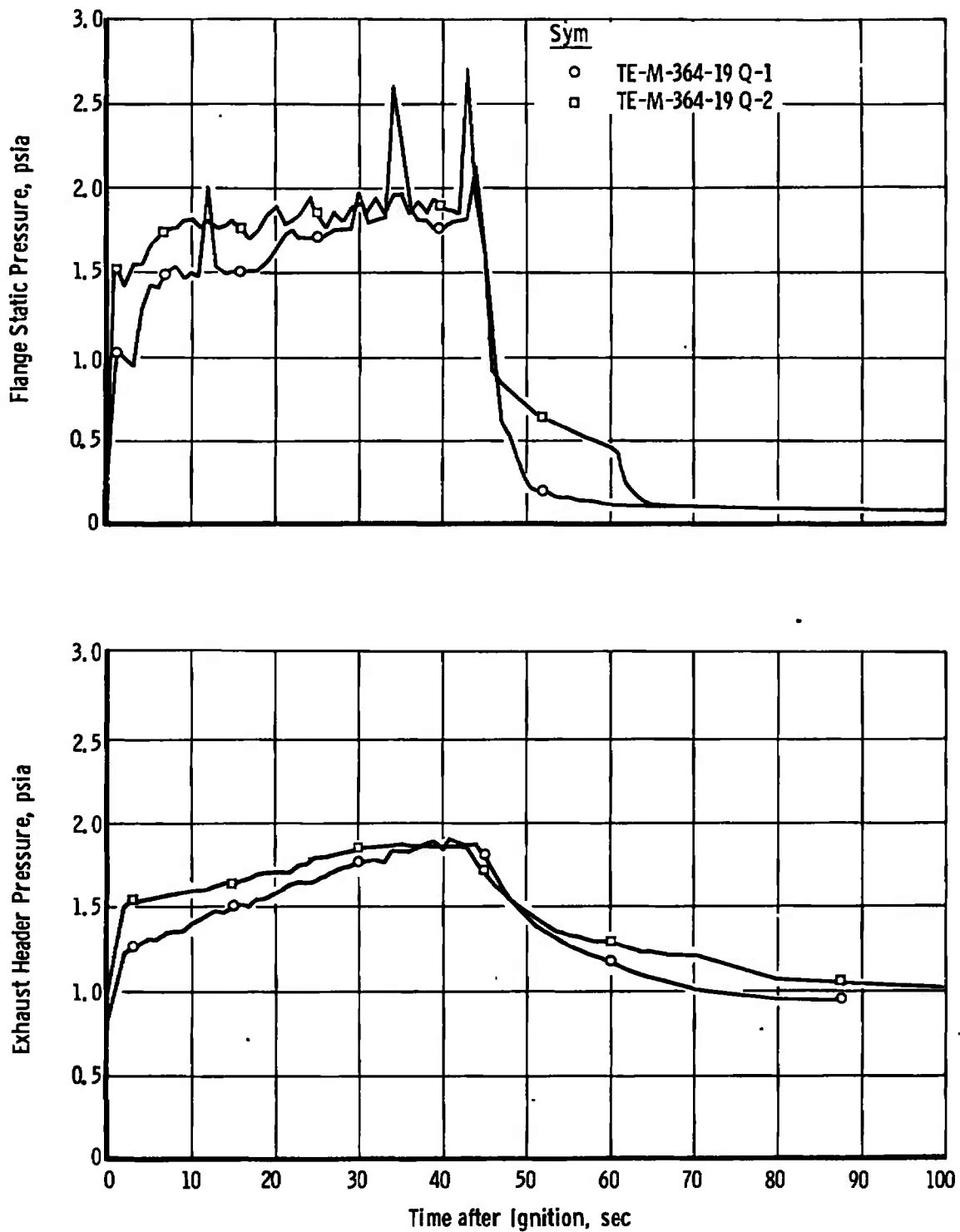
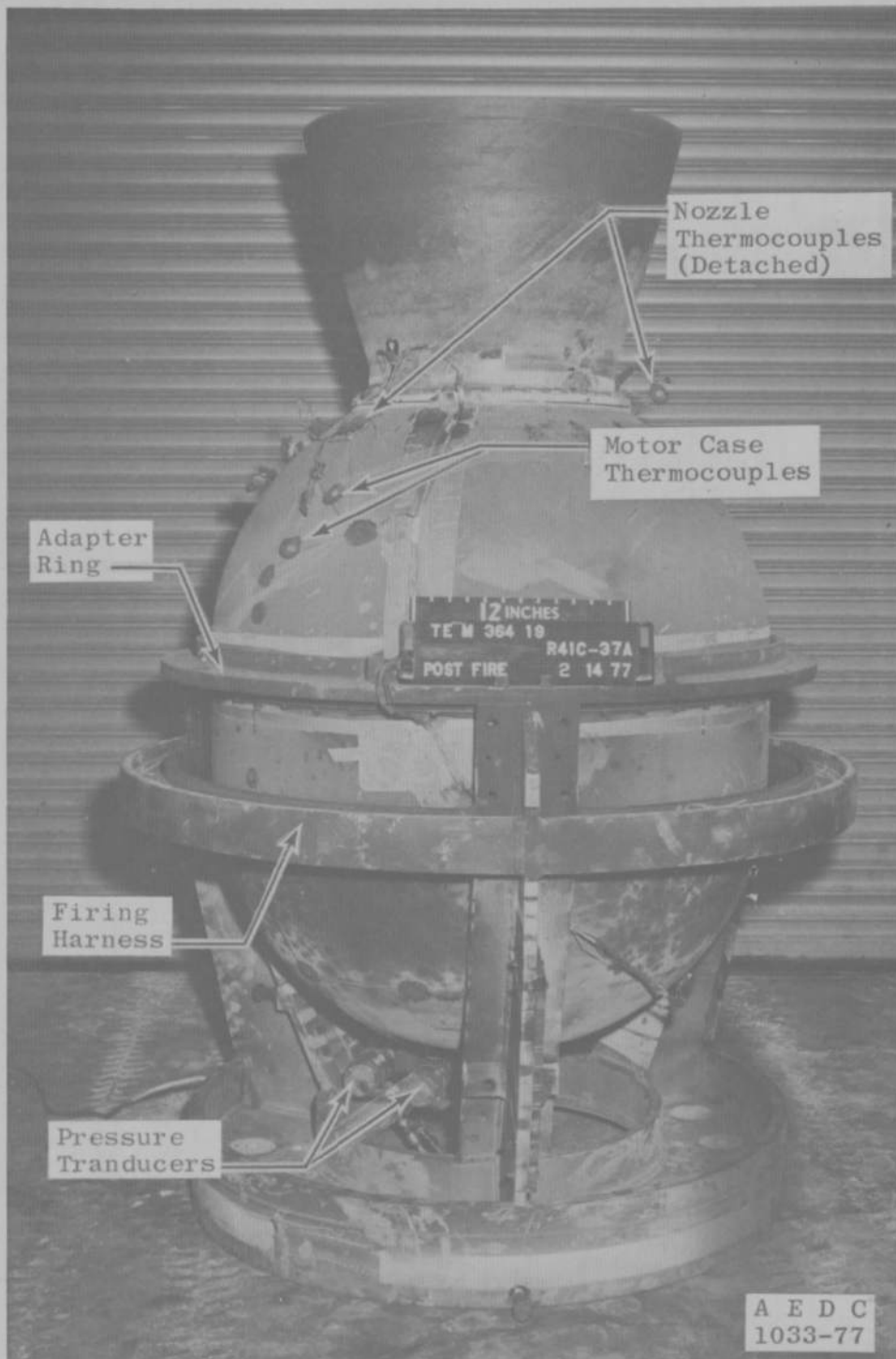
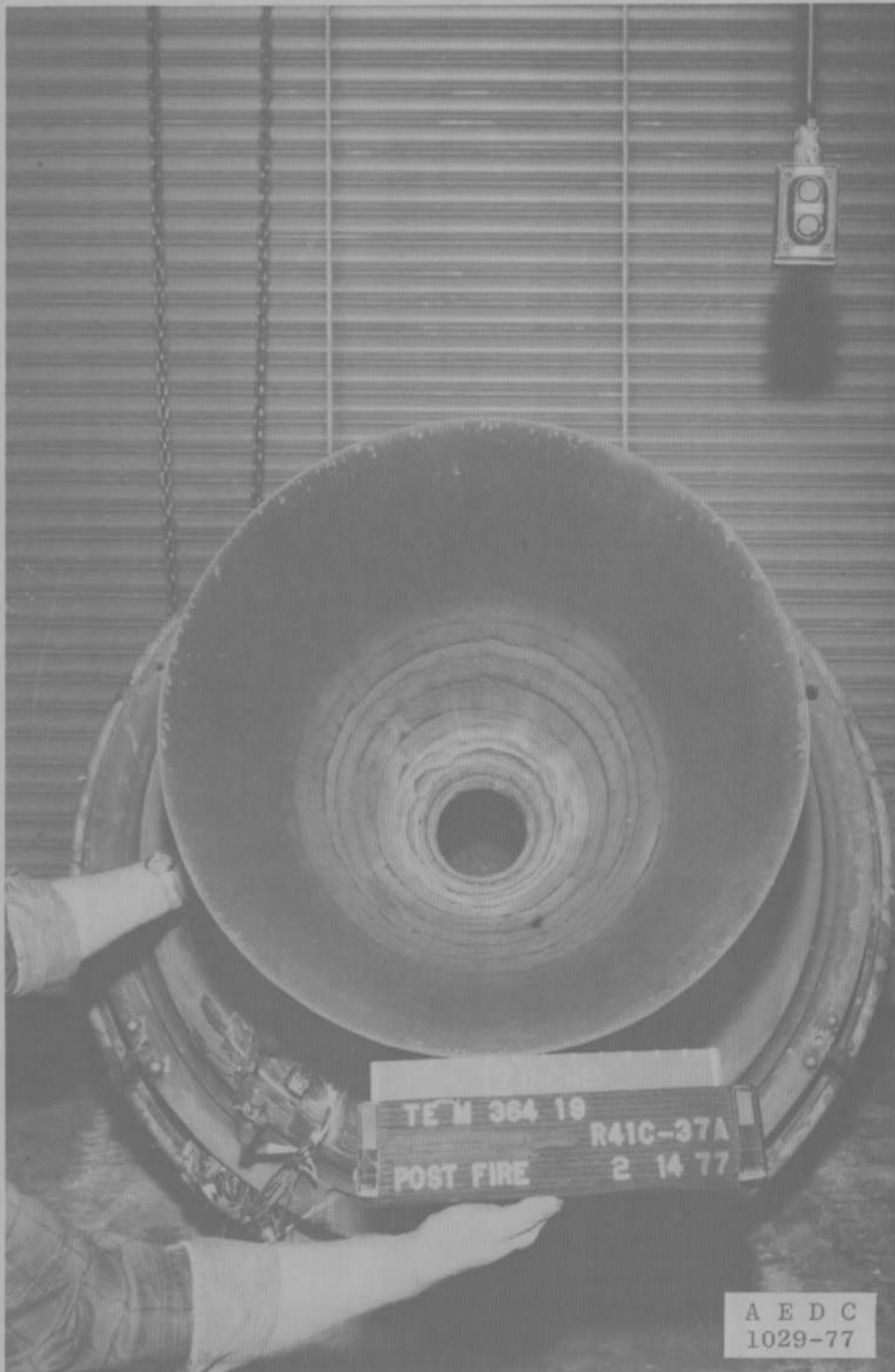


Figure 6. Comparison of exhaust ducting pressures during firing.

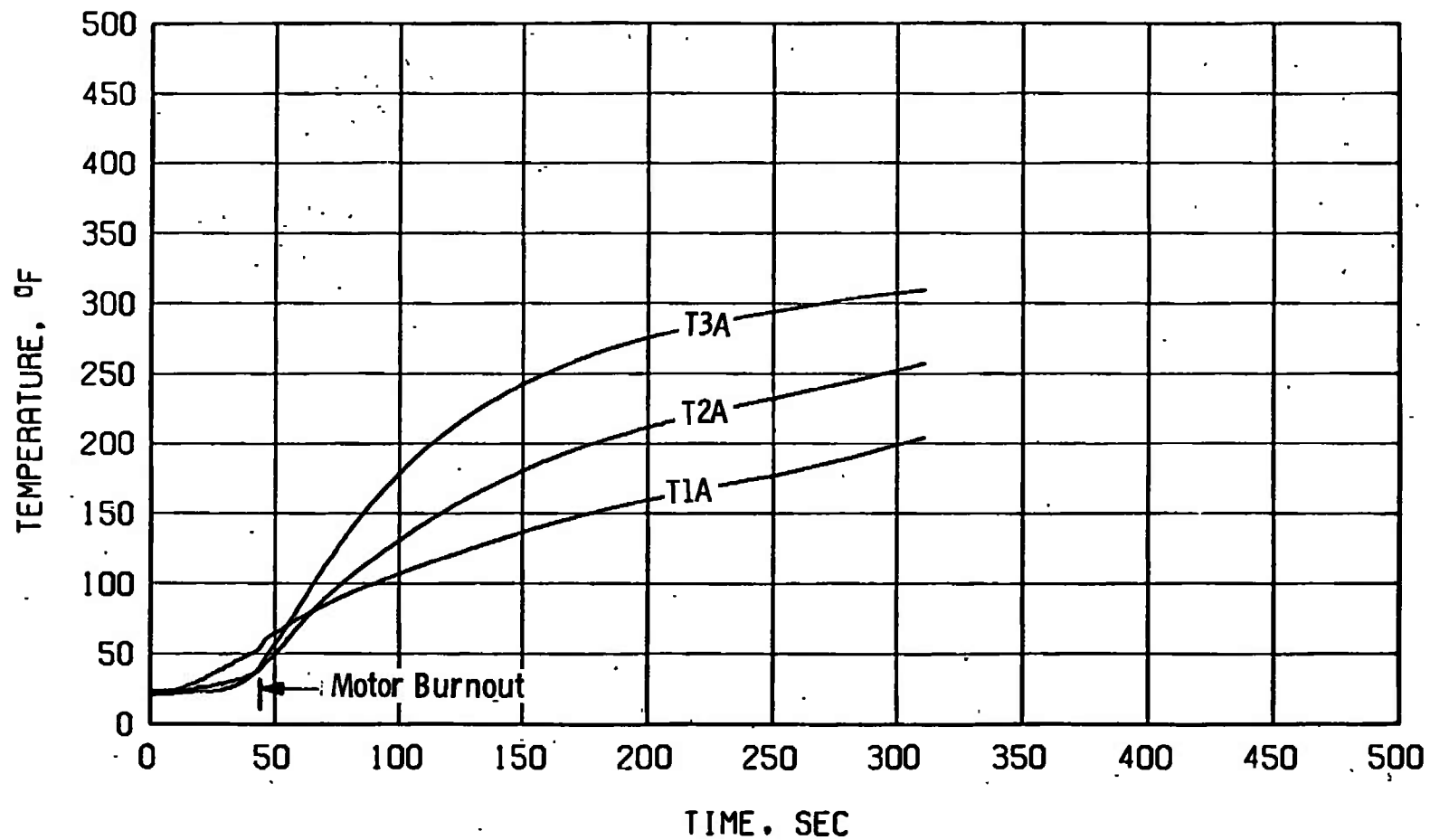


a. Motor case and nozzle

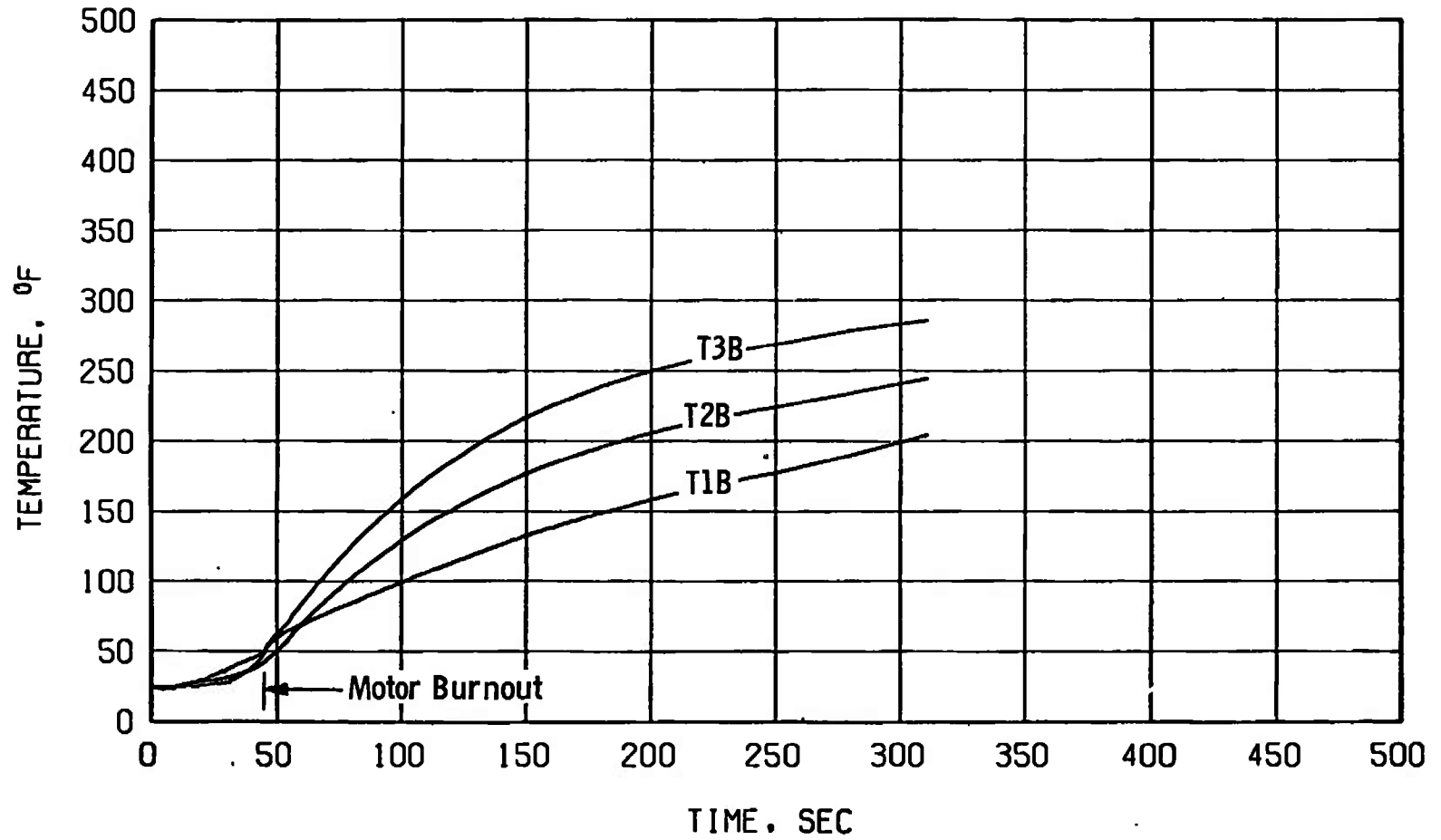
Figure 7. Postfire photograph of motor assembly.



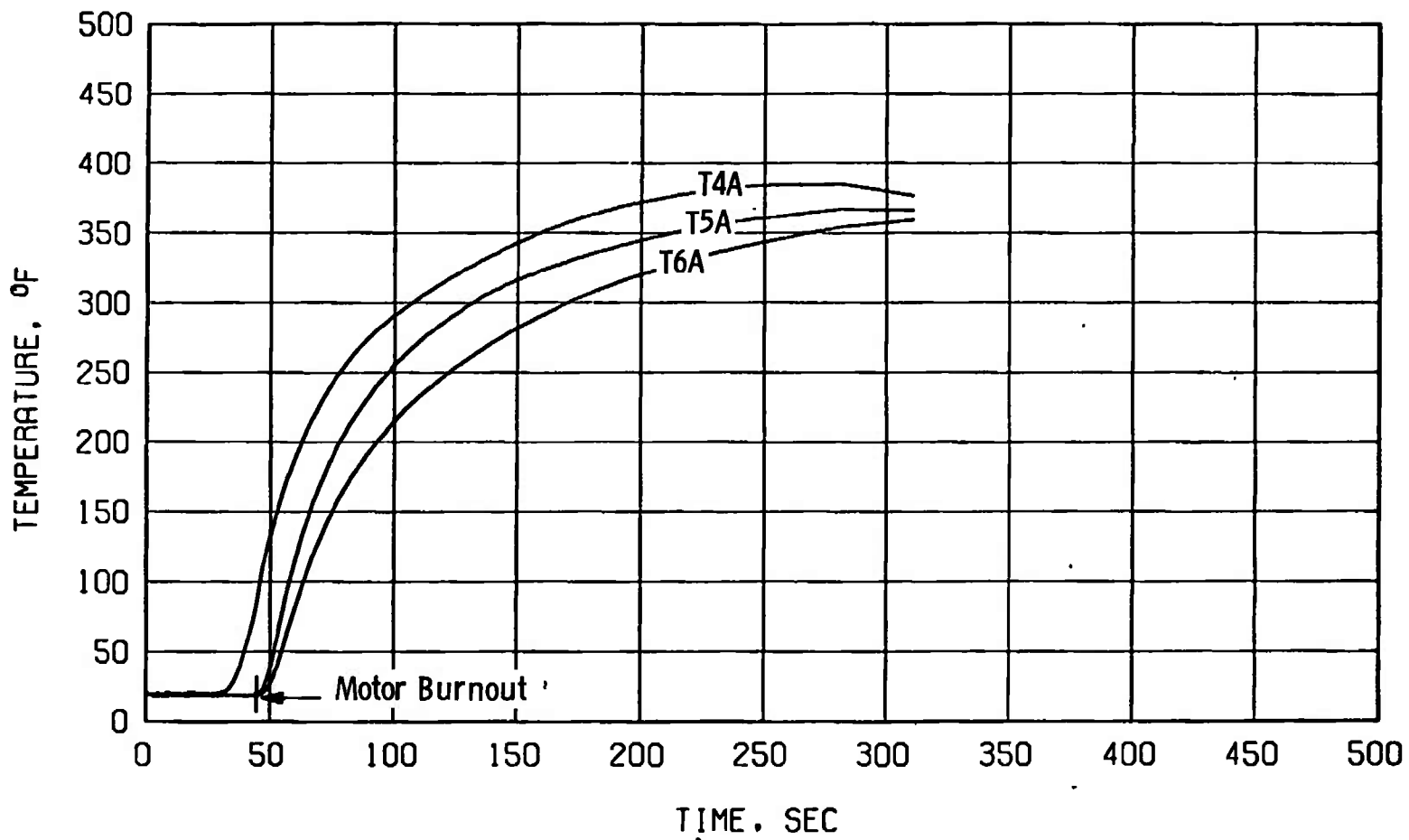
b. Nozzle interior
Figure 7. Concluded.



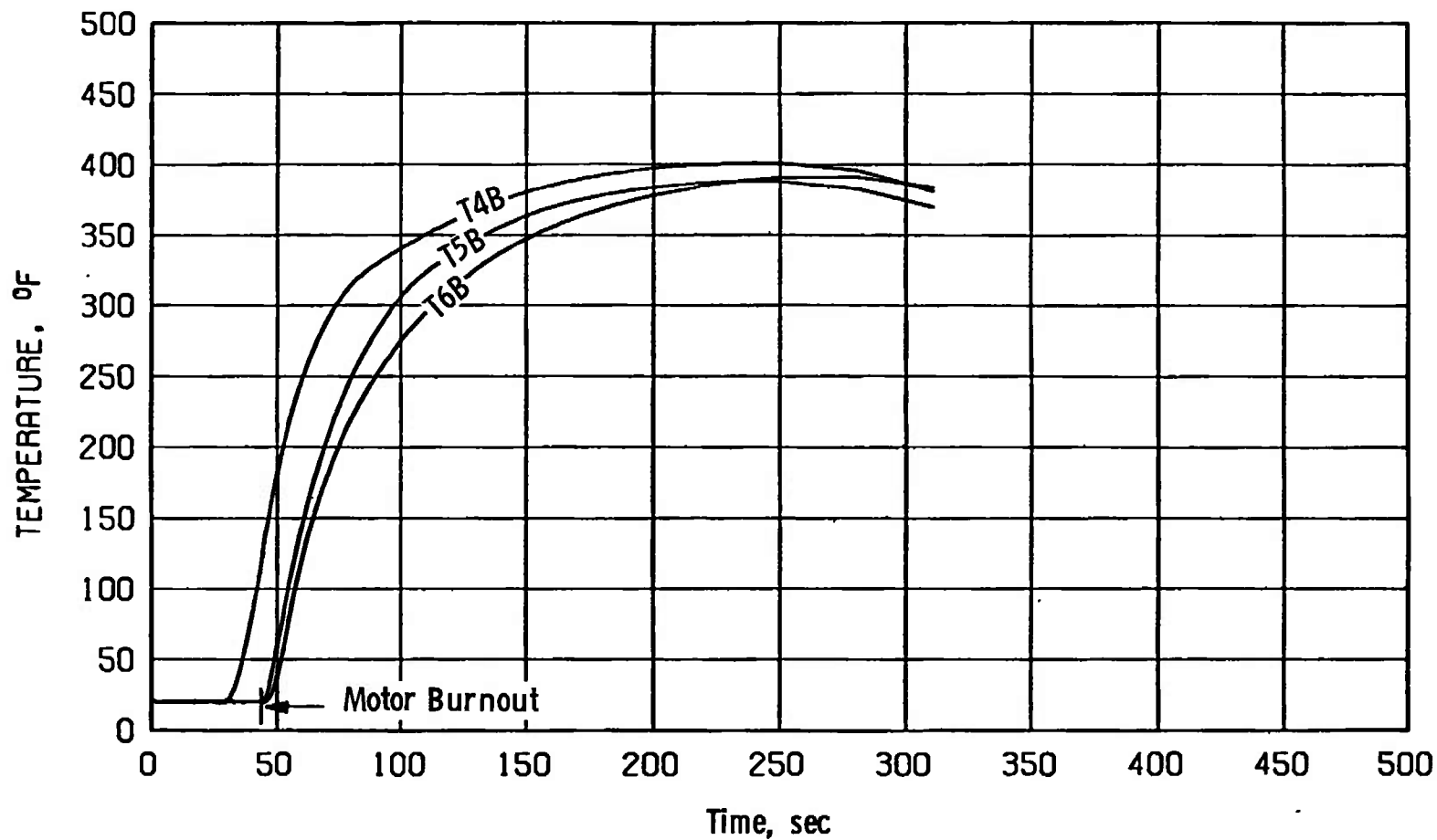
a. Case thermocouples T1A, T2A, and T3A
Figure 8. Motor temperature variation with time.



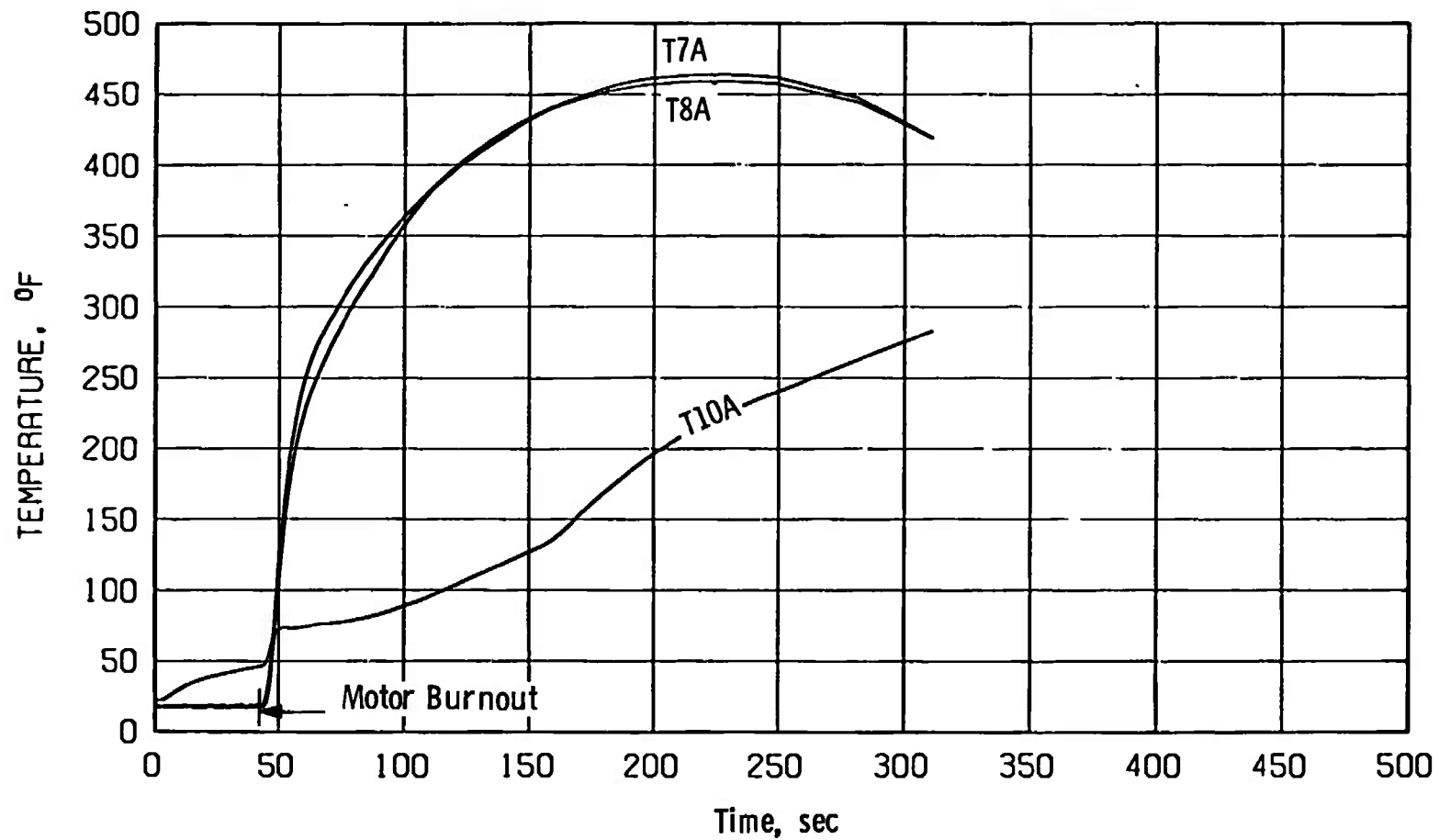
b. Case thermocouples T1B, T2B, and T3B
Figure 8. Continued.



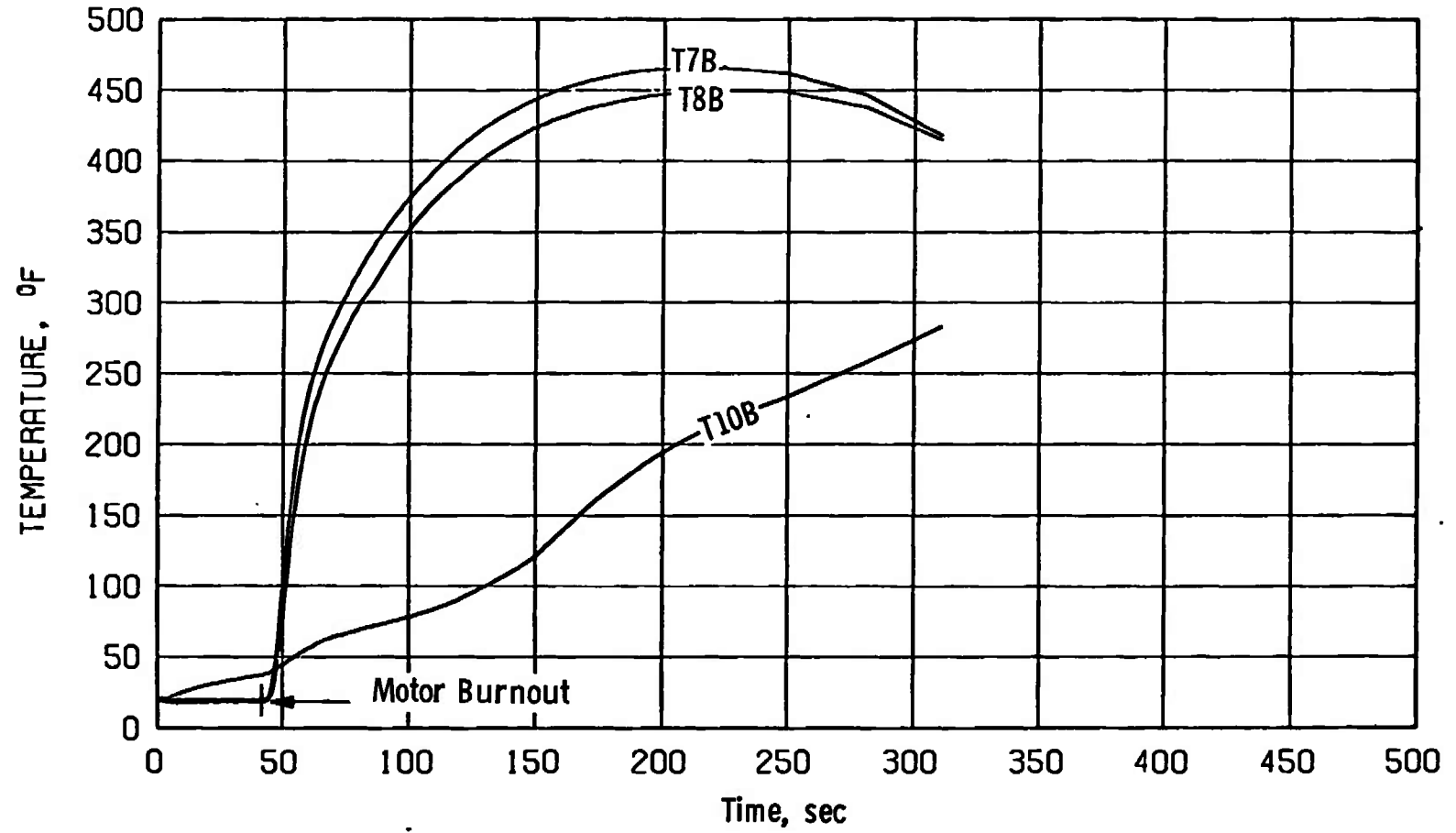
c. Case thermocouples T4A, T5A, and T6A
Figure 8. Continued.



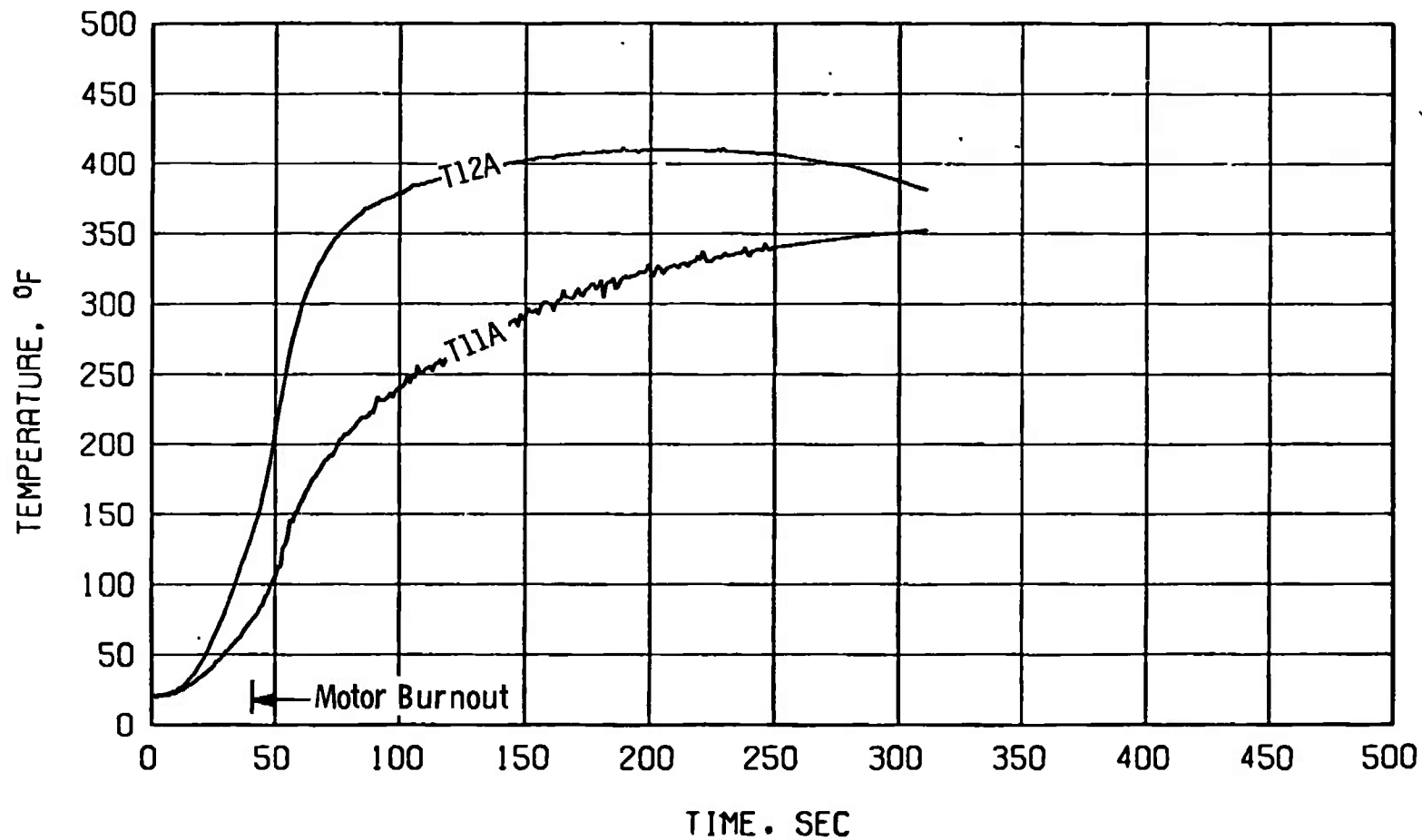
d. Case thermocouples T4B, T5B, and T6B
Figure 8. Continued.



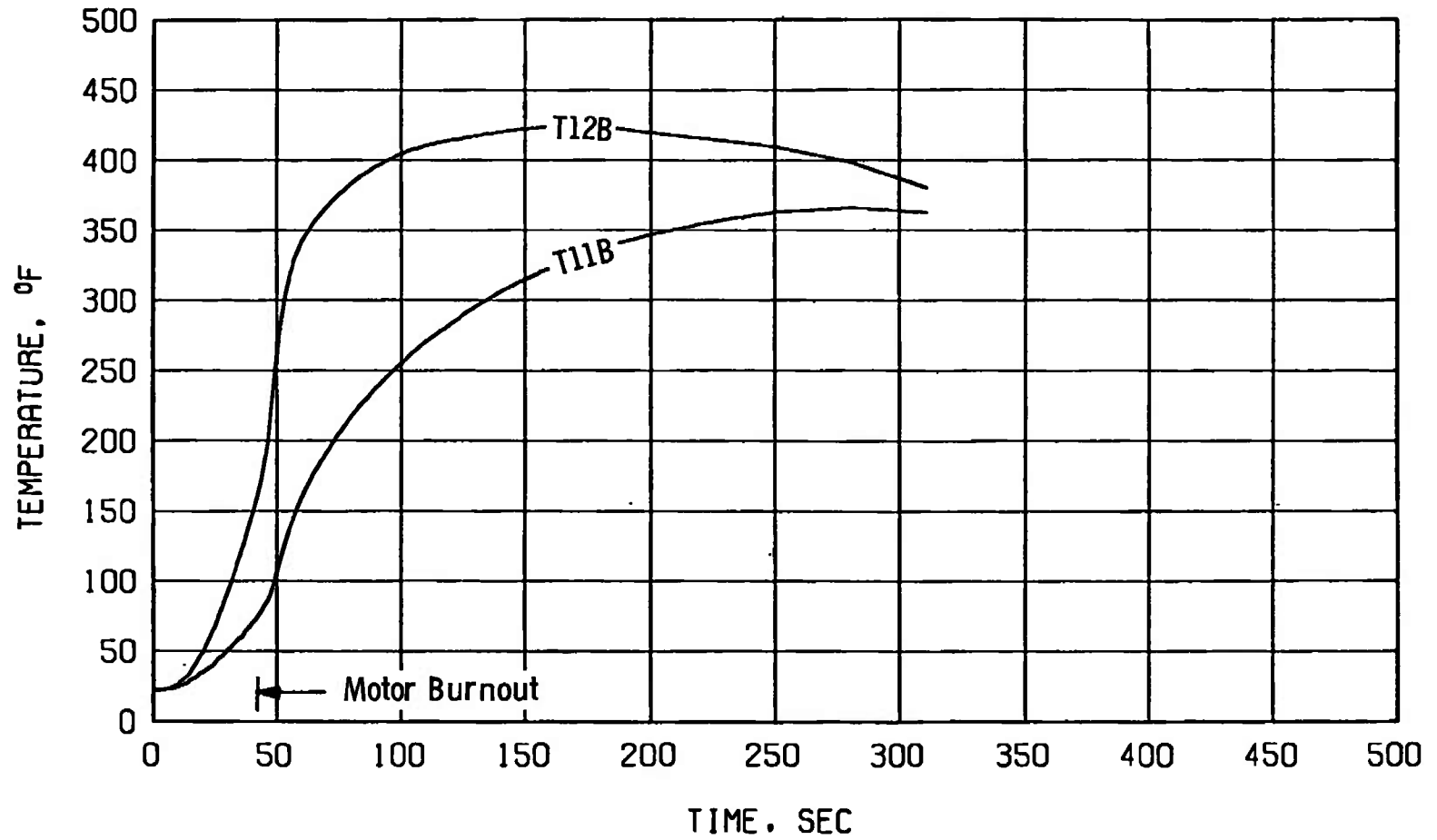
e. Case thermocouples T7A, T8A, and T10A
Figure 8. Continued.



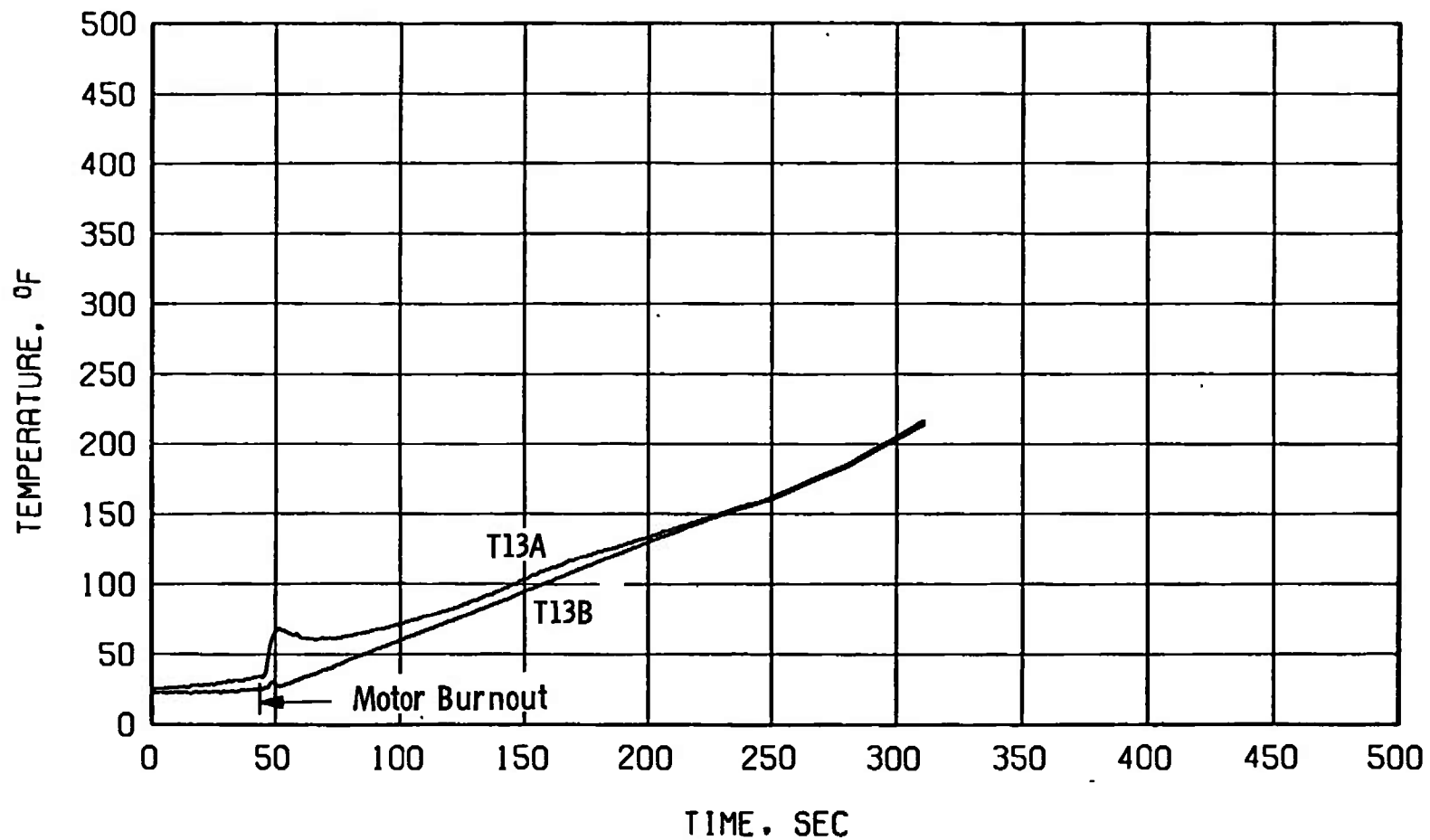
f. Case thermocouples T7B, T8B, and T10B
Figure 8. Continued.



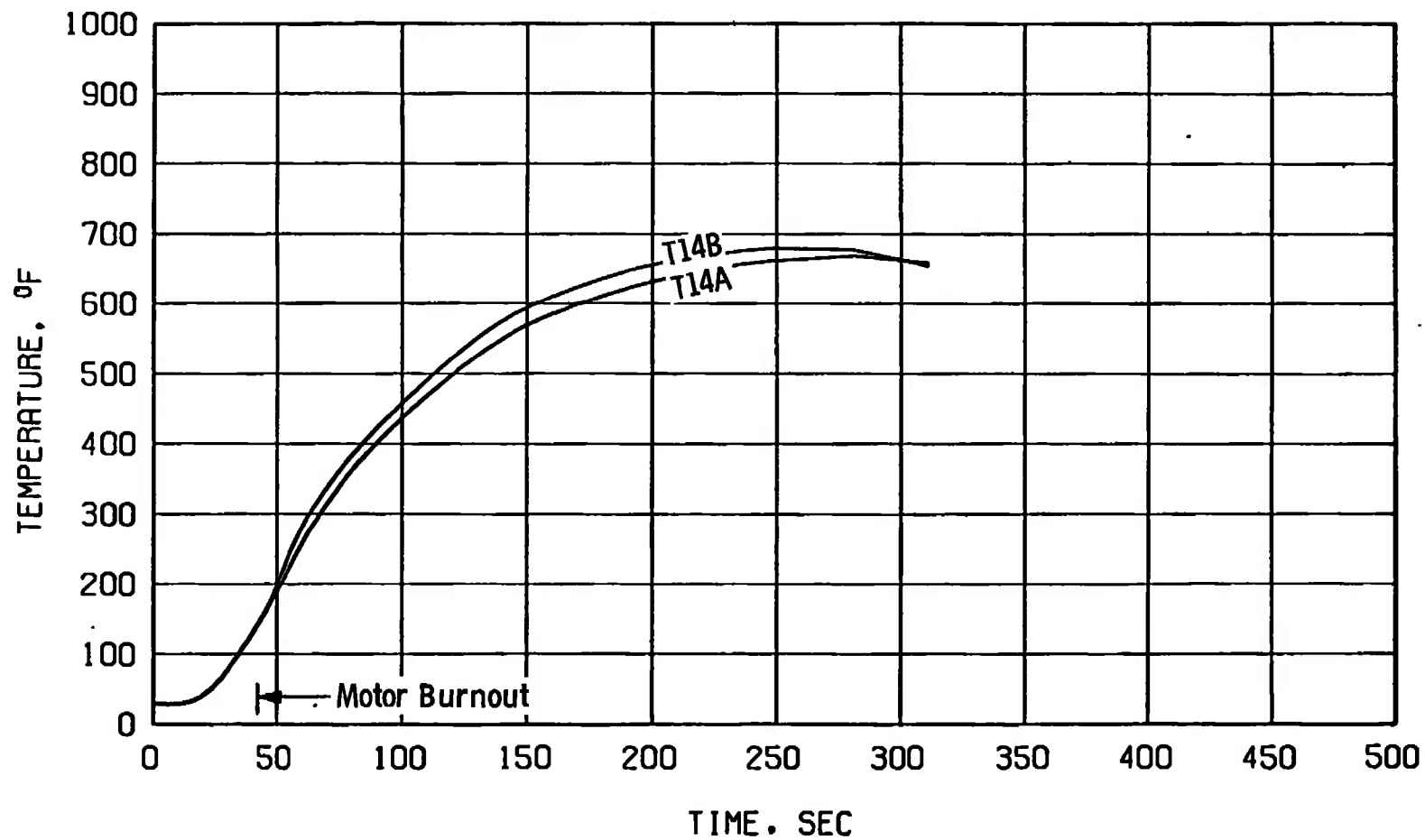
g. Case thermocouples T11A and T12A
Figure 8. Continued.



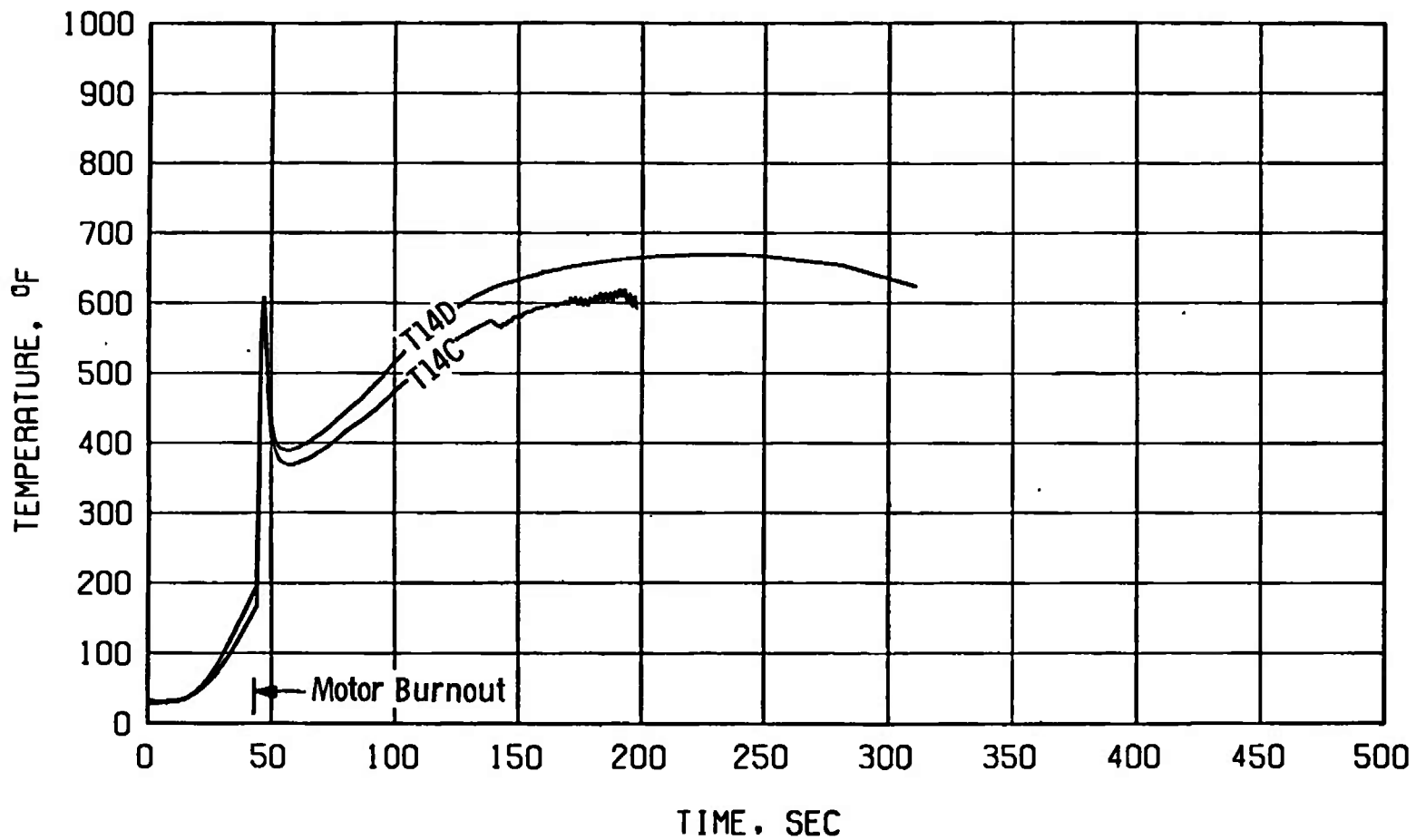
h. Case thermocouples T11B and T12B
Figure 8. Continued.



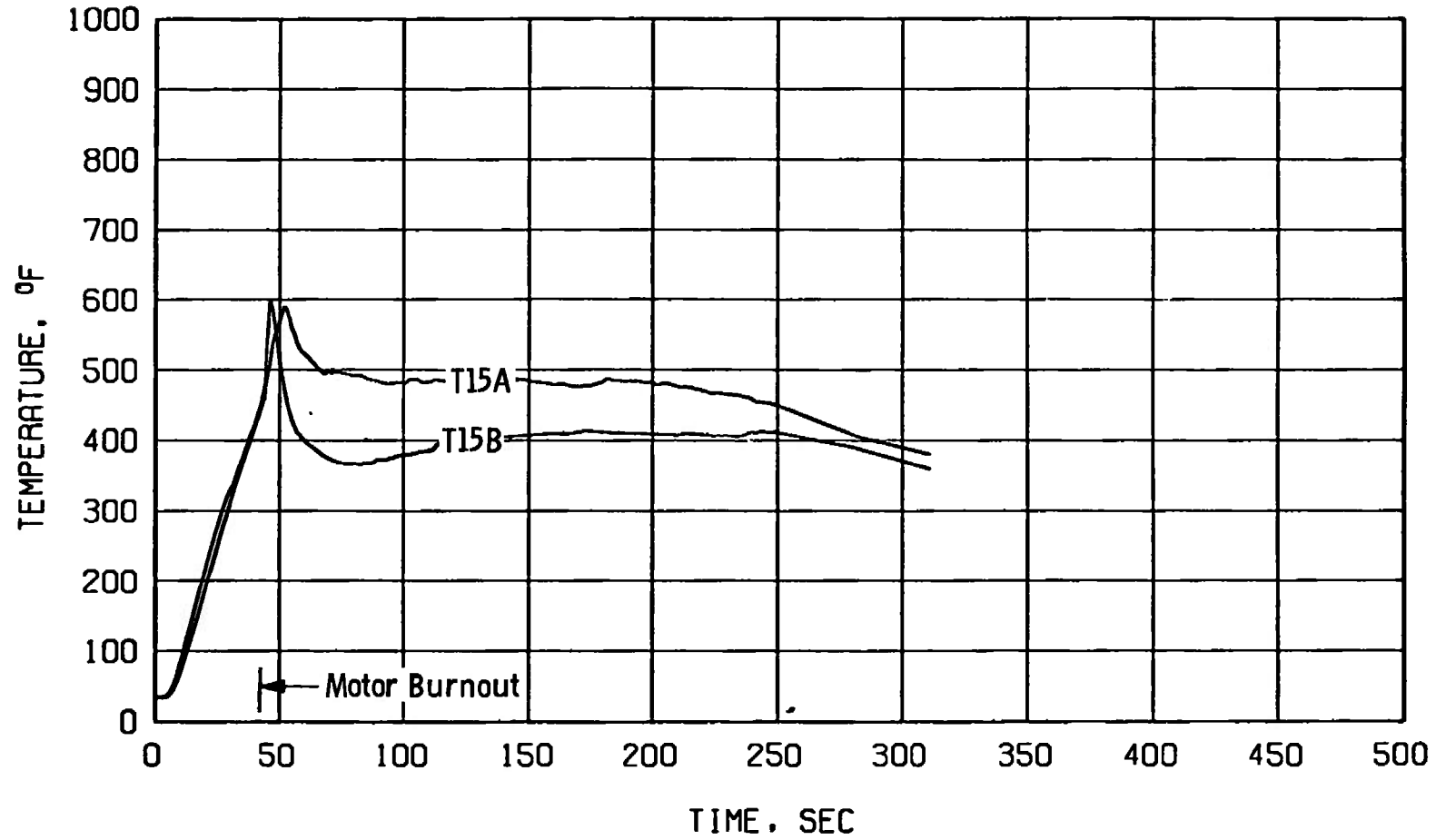
i. Nozzle thermocouples T13A and T13B
Figure 8. Continued.



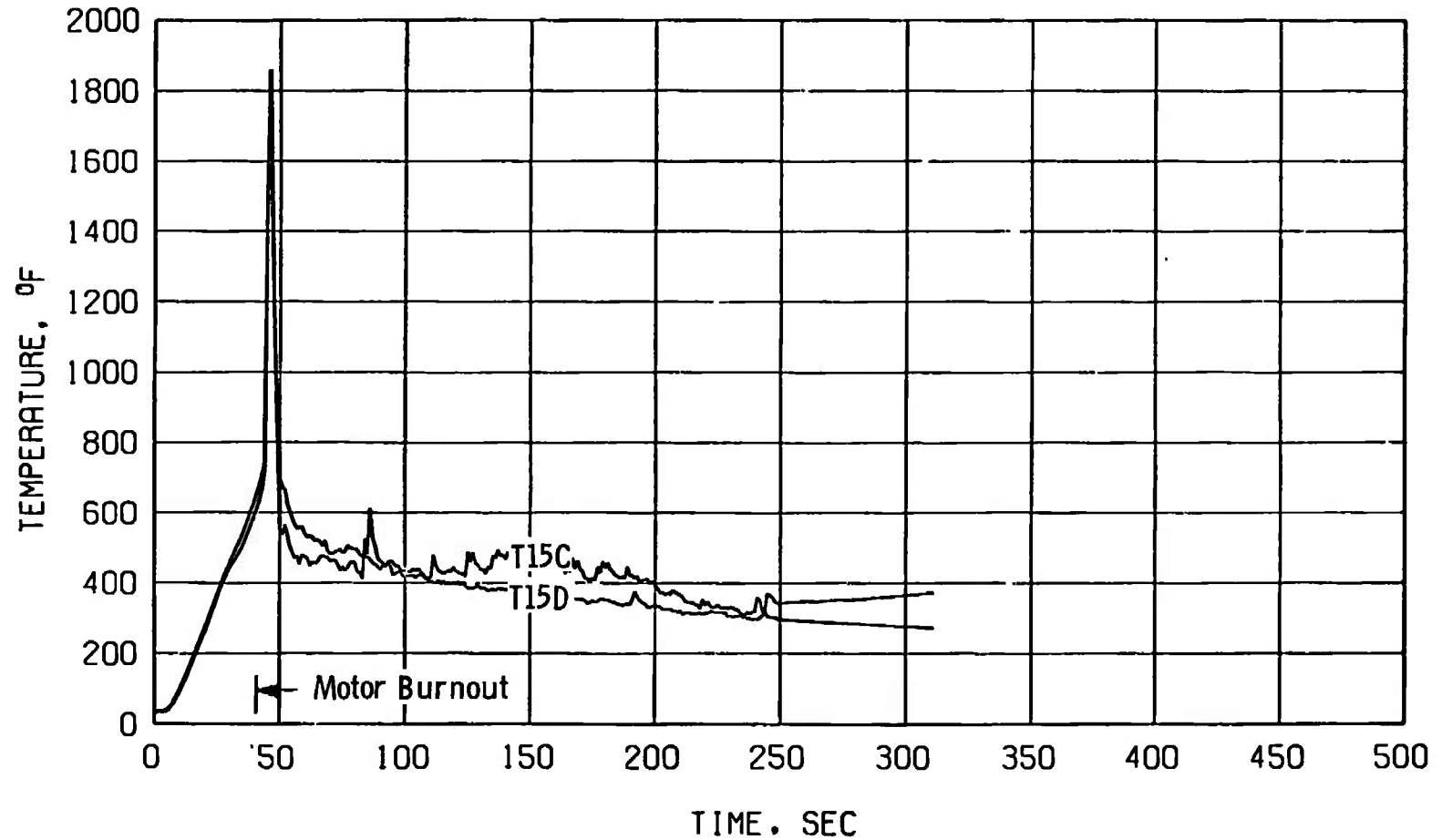
j. Nozzle thermocouples T14A and T14B
Figure 8. Continued.



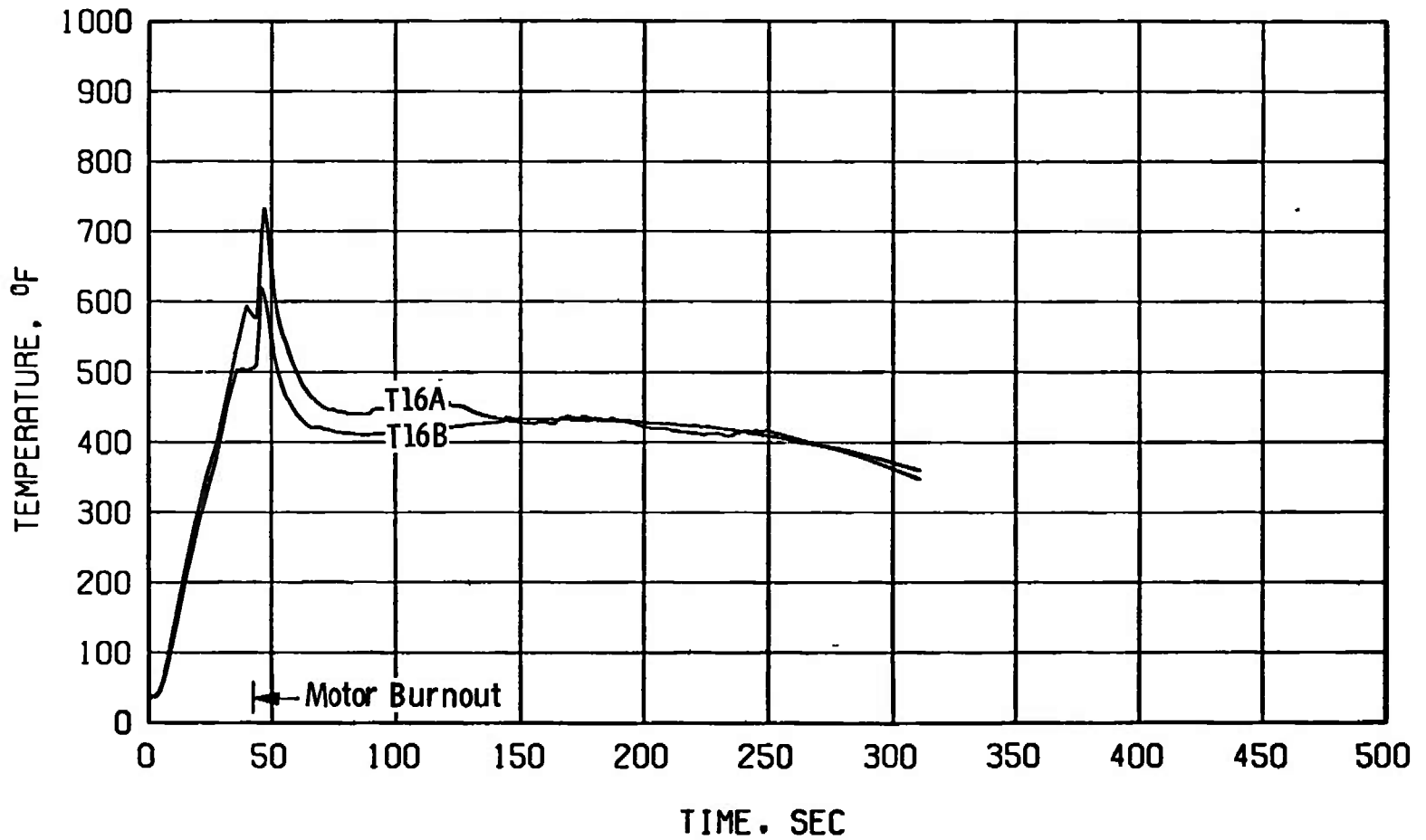
k. Nozzle thermocouples T14C and T14D
Figure 8. Continued.



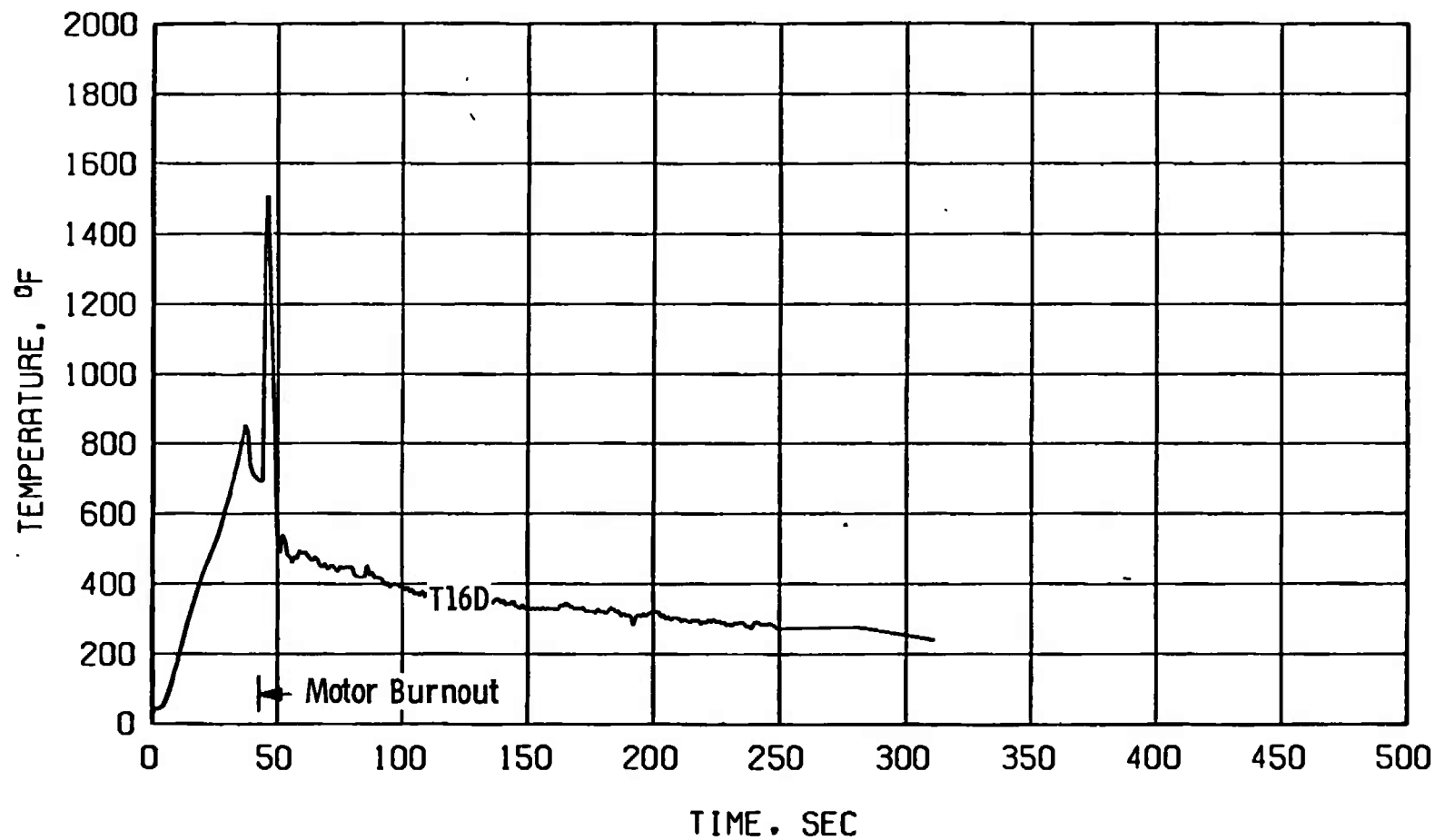
I. Nozzle thermocouples T15A and T15B
Figure 8. Continued.



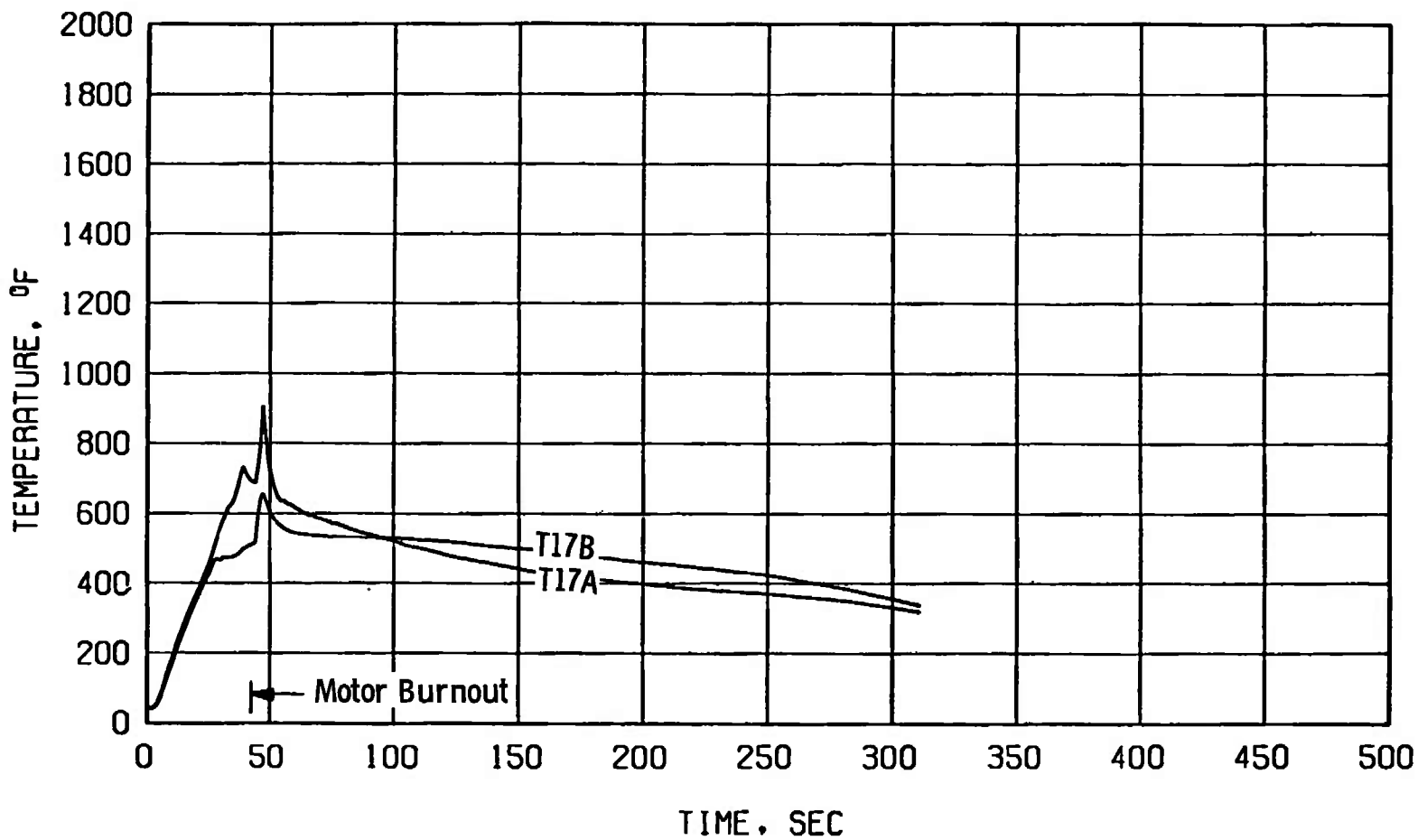
m. Nozzle thermocouples T15C and T15D
Figure 8. Continued.



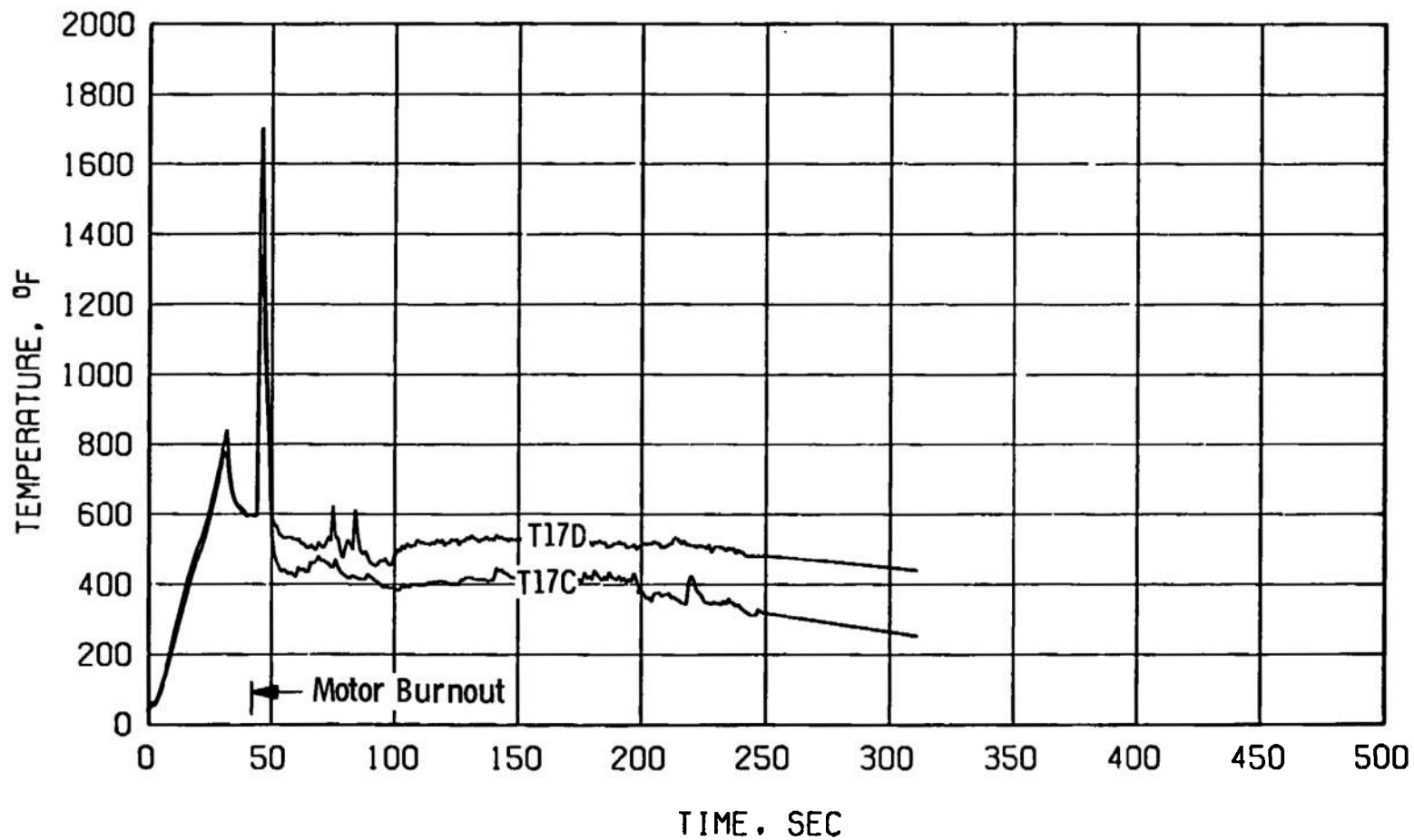
n. Nozzle thermocouples T16A and T16B
Figure 8. Continued.



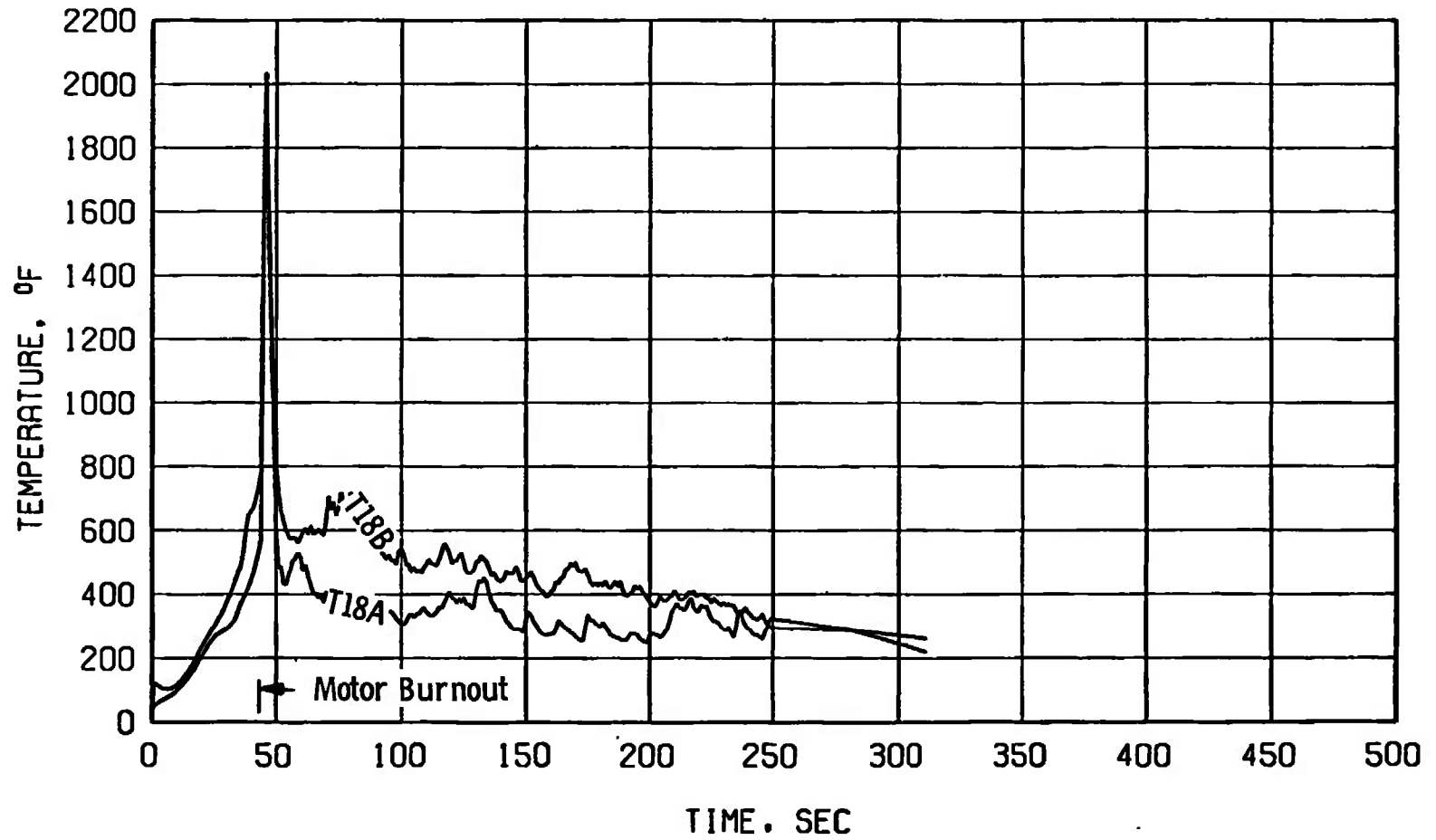
o. Nozzle thermocouple T16D
Figure 8. Continued.



p. Nozzle thermocouples T17A and T17B
Figure 8. Continued.



q. Nozzle thermocouples T17C and T17D
Figure 8. Continued.



r. Nozzle thermocouples T18A and T18B
Figure 8. Concluded.

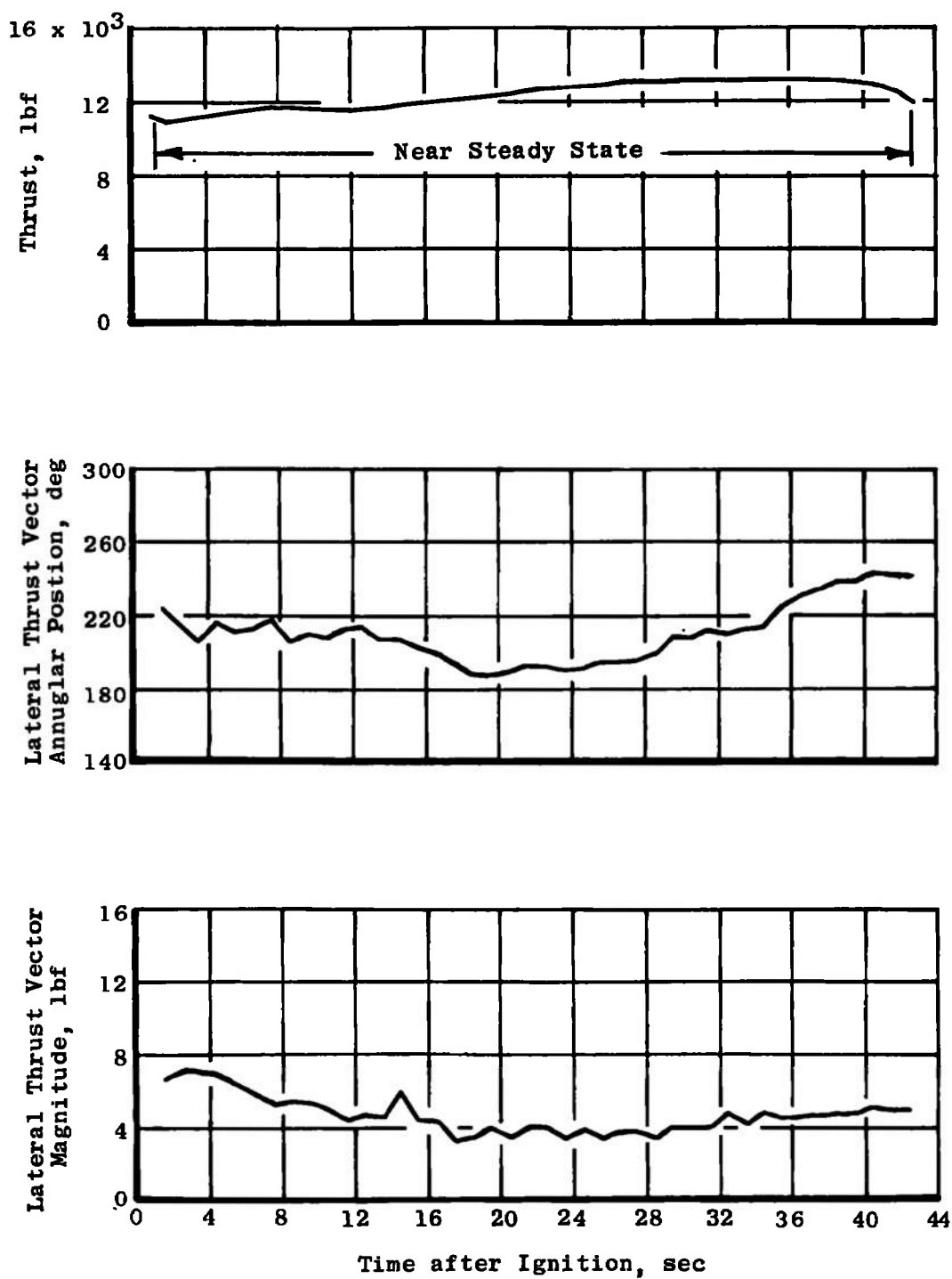
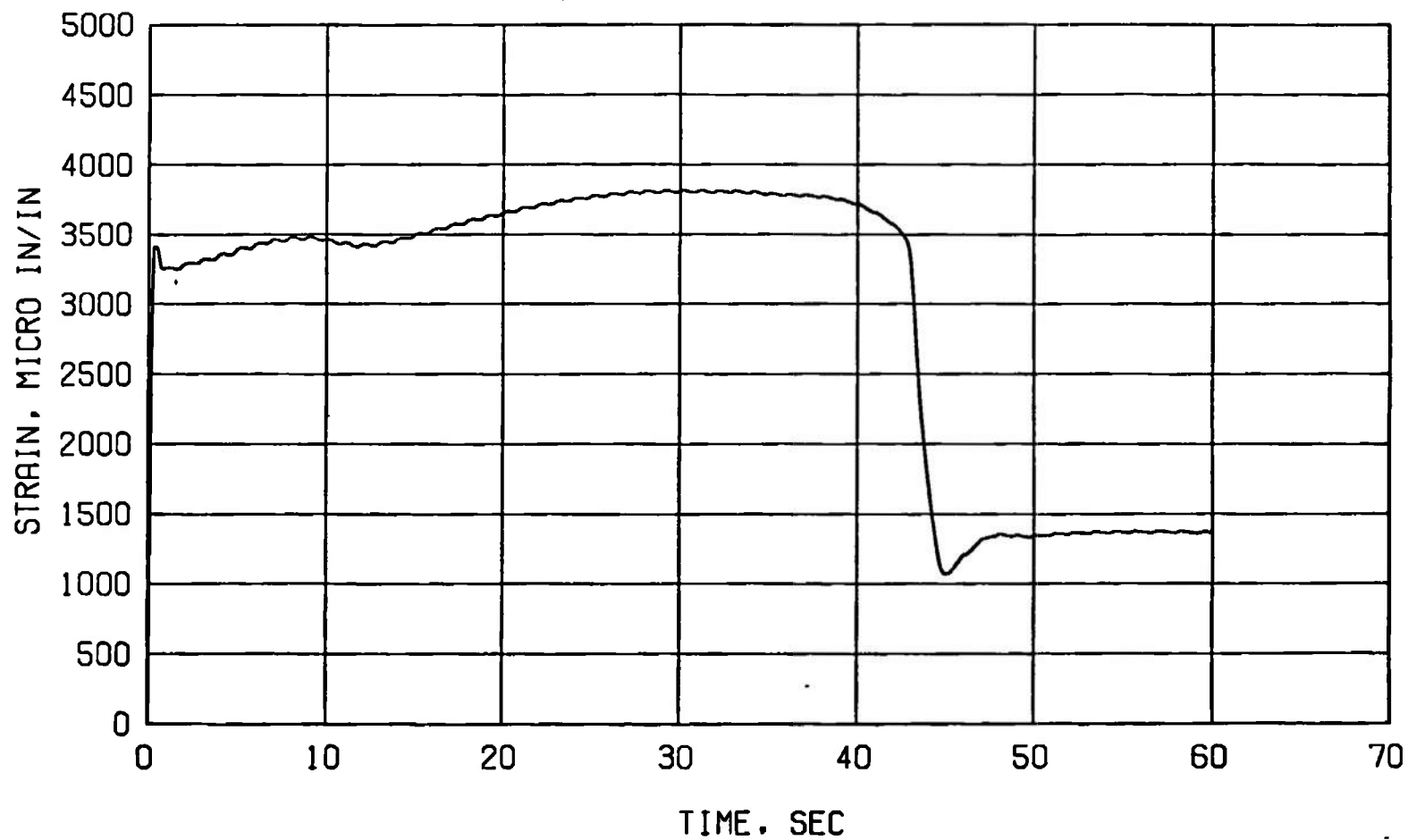
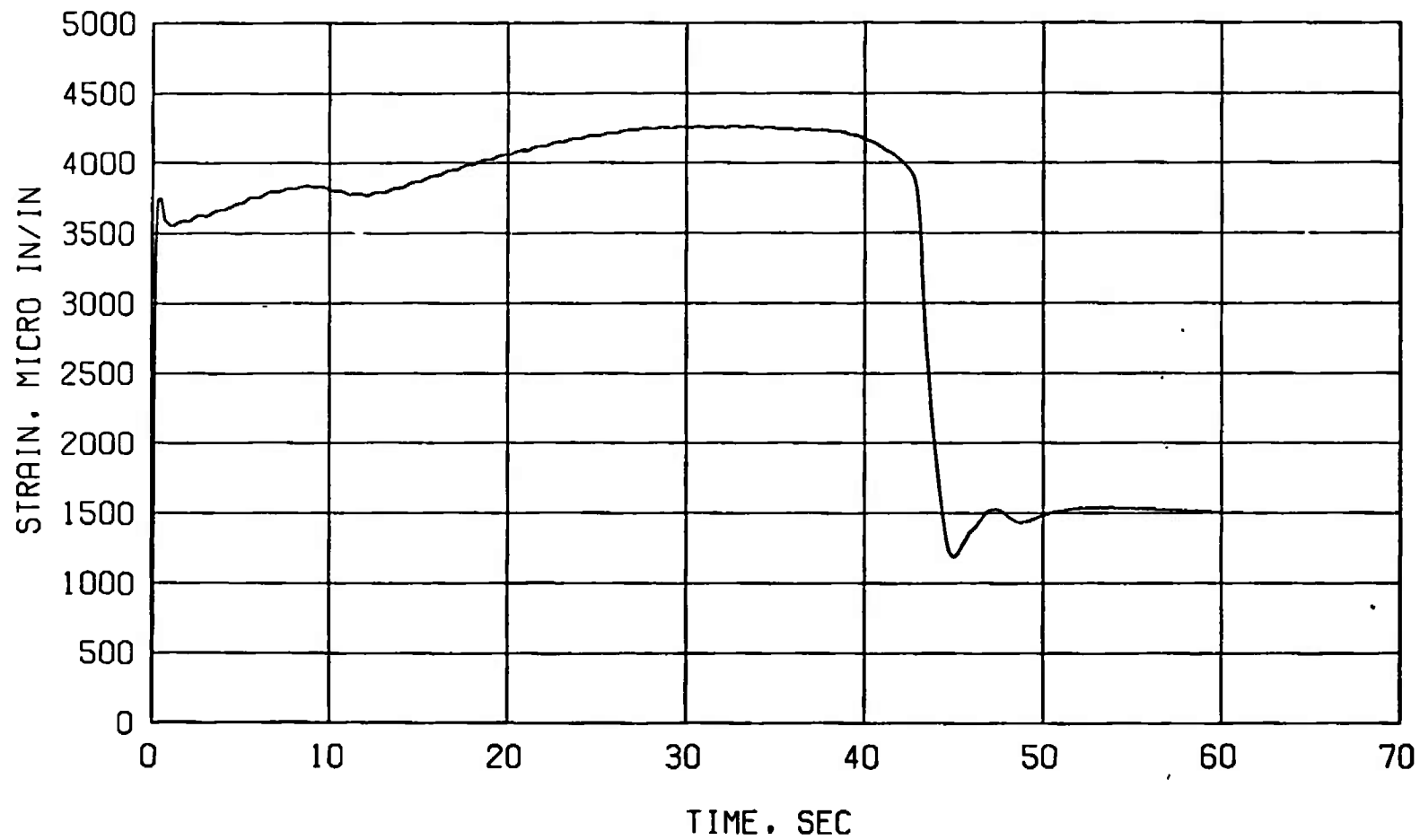


Figure 9. Variation of lateral (nonaxial) thrust vector during firing.

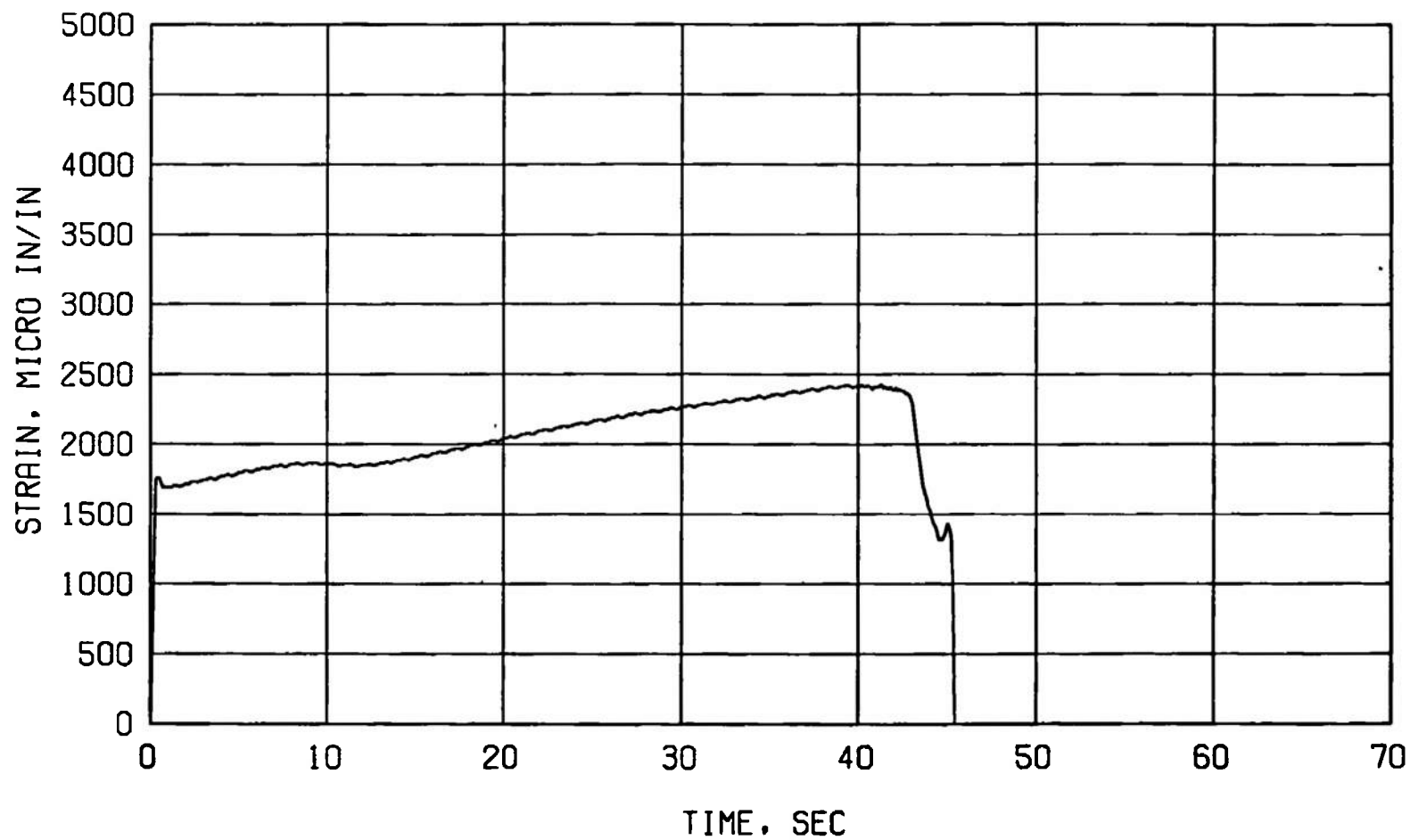


a. Case strain 2A

Figure 10. Variation of motor case strain during firing.

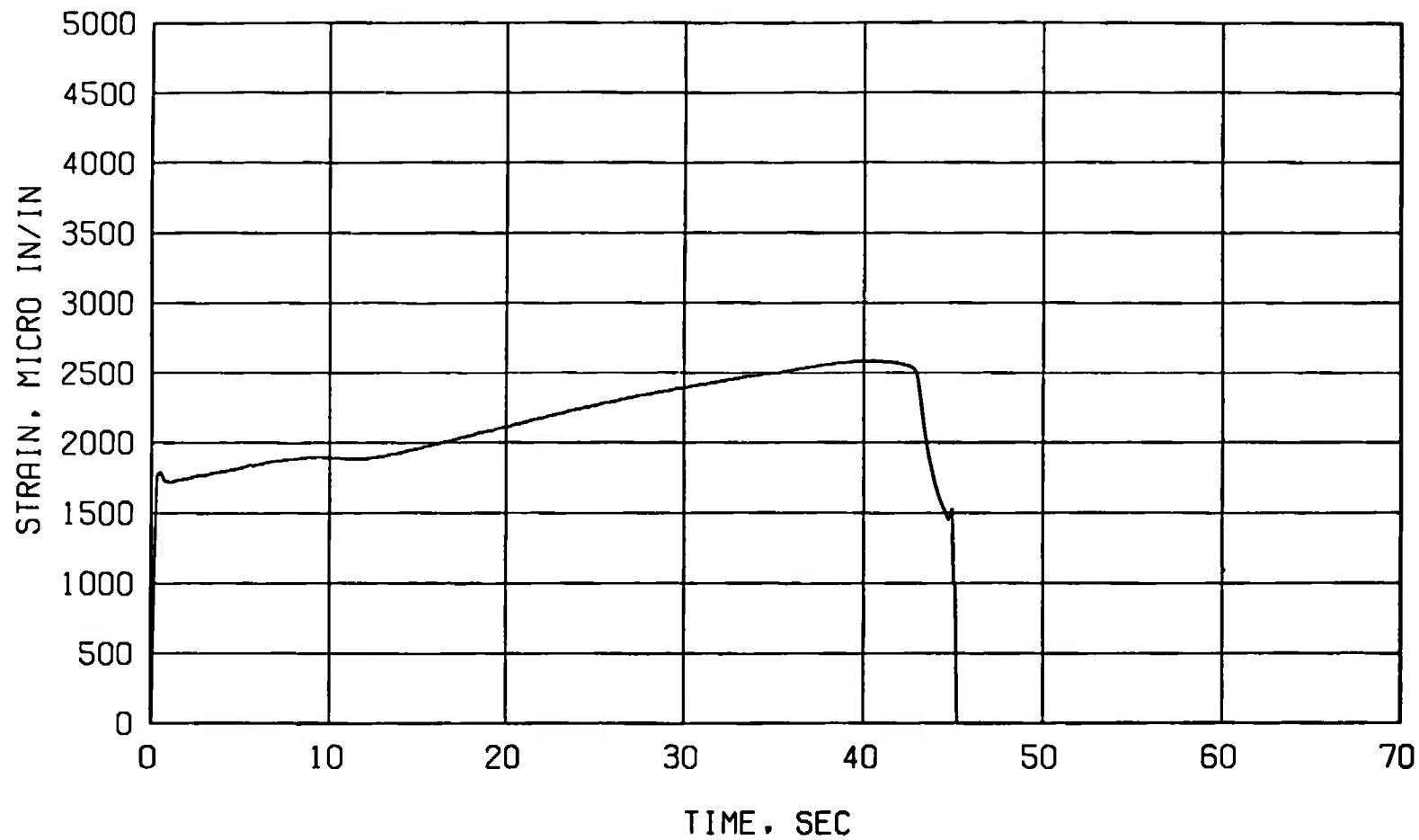


b. Case strain 2B
Figure 10. Concluded.

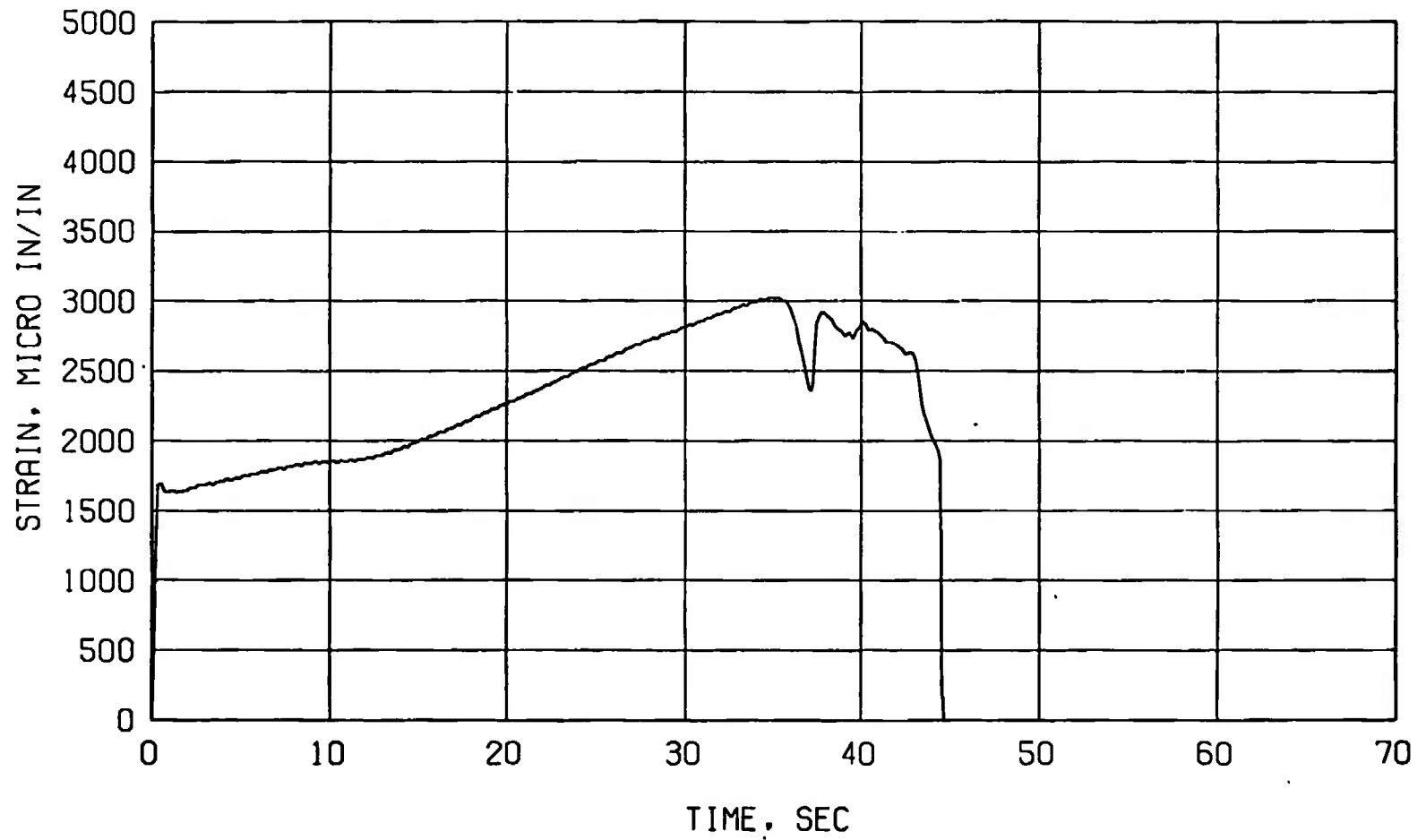


a. Nozzle strain 3A

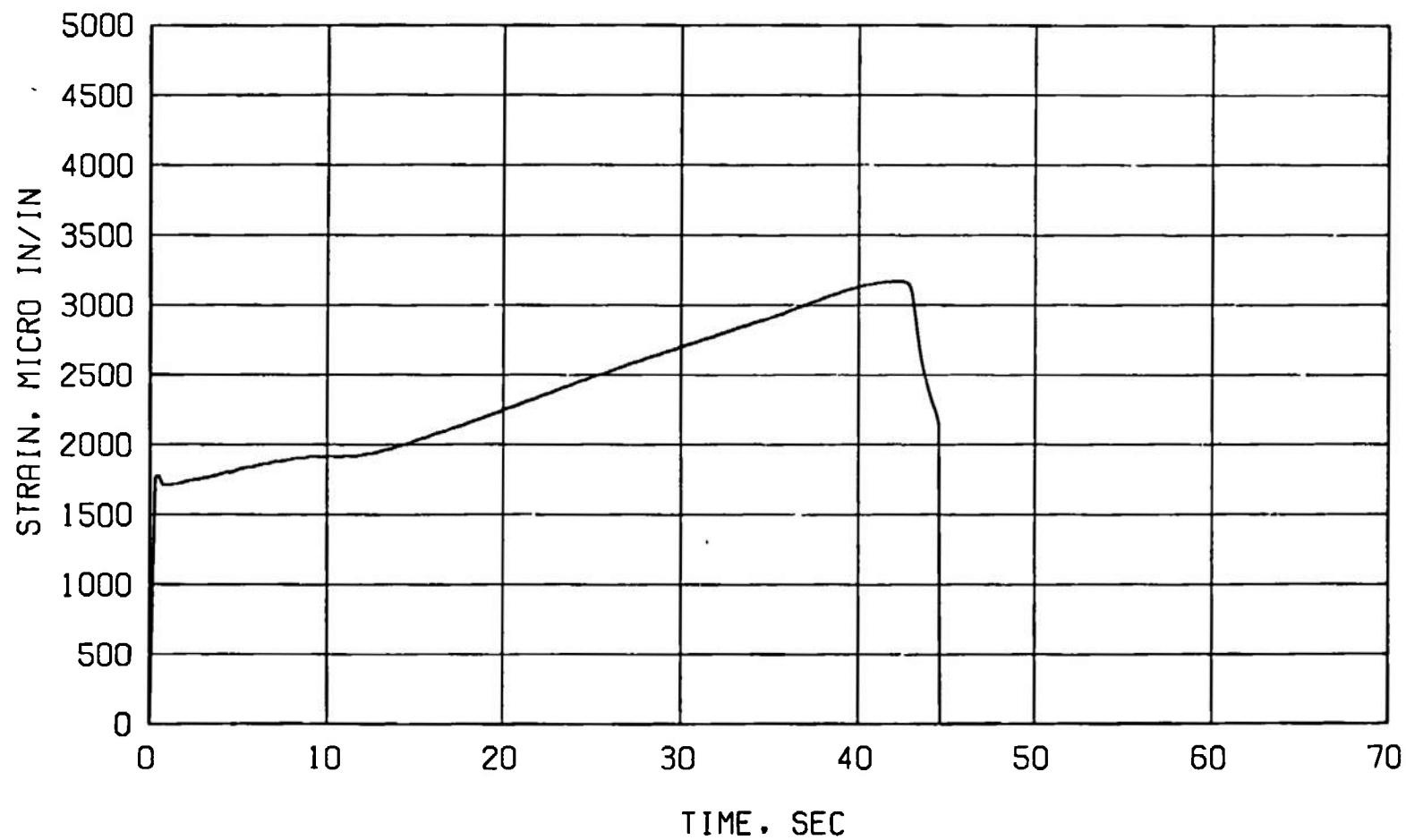
Figure 11. Variation of nozzle adapter flange strain during firing.



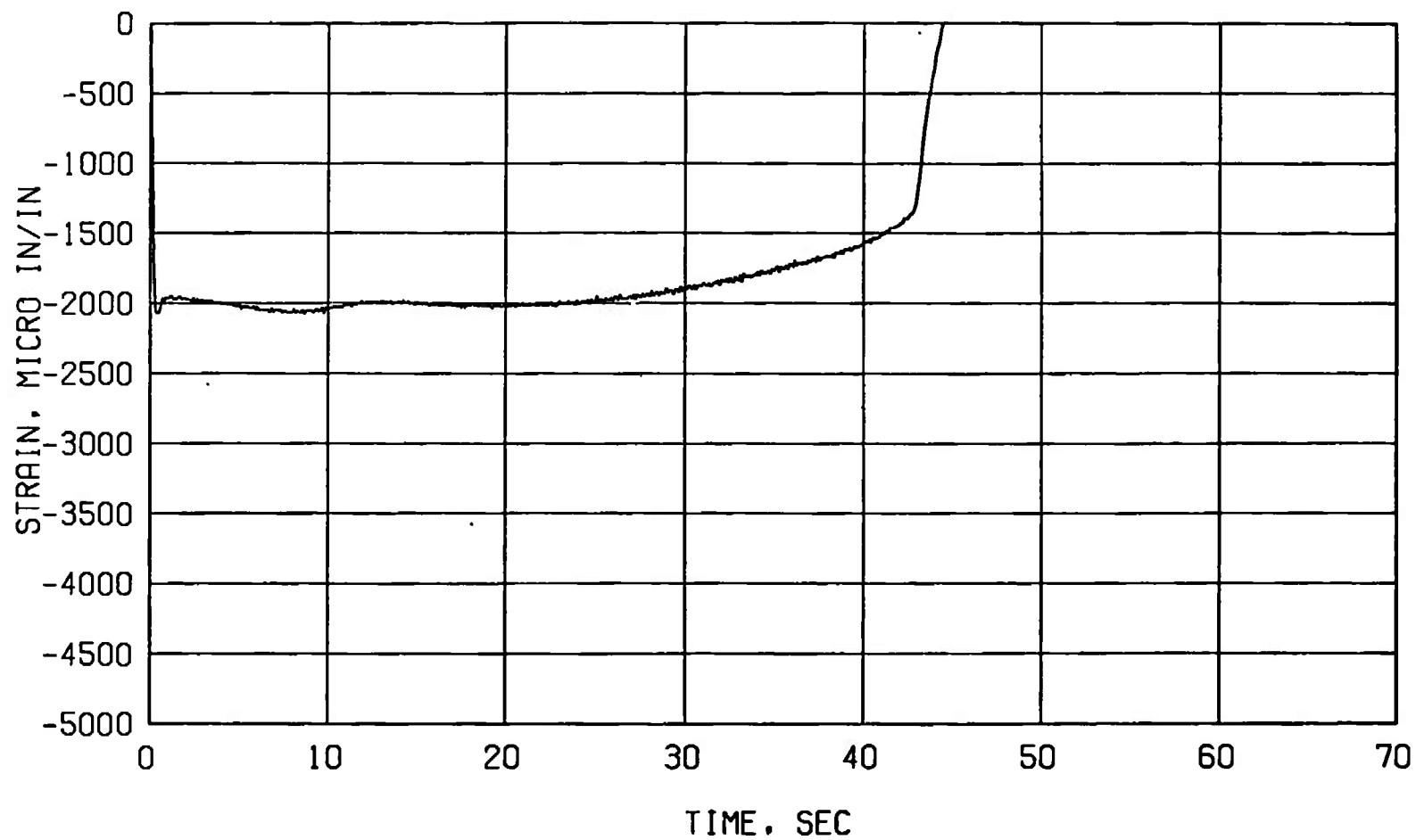
b. Nozzle strain 3B
Figure 11. Continued.



c. Nozzle strain 3C
Figure 11. Continued.

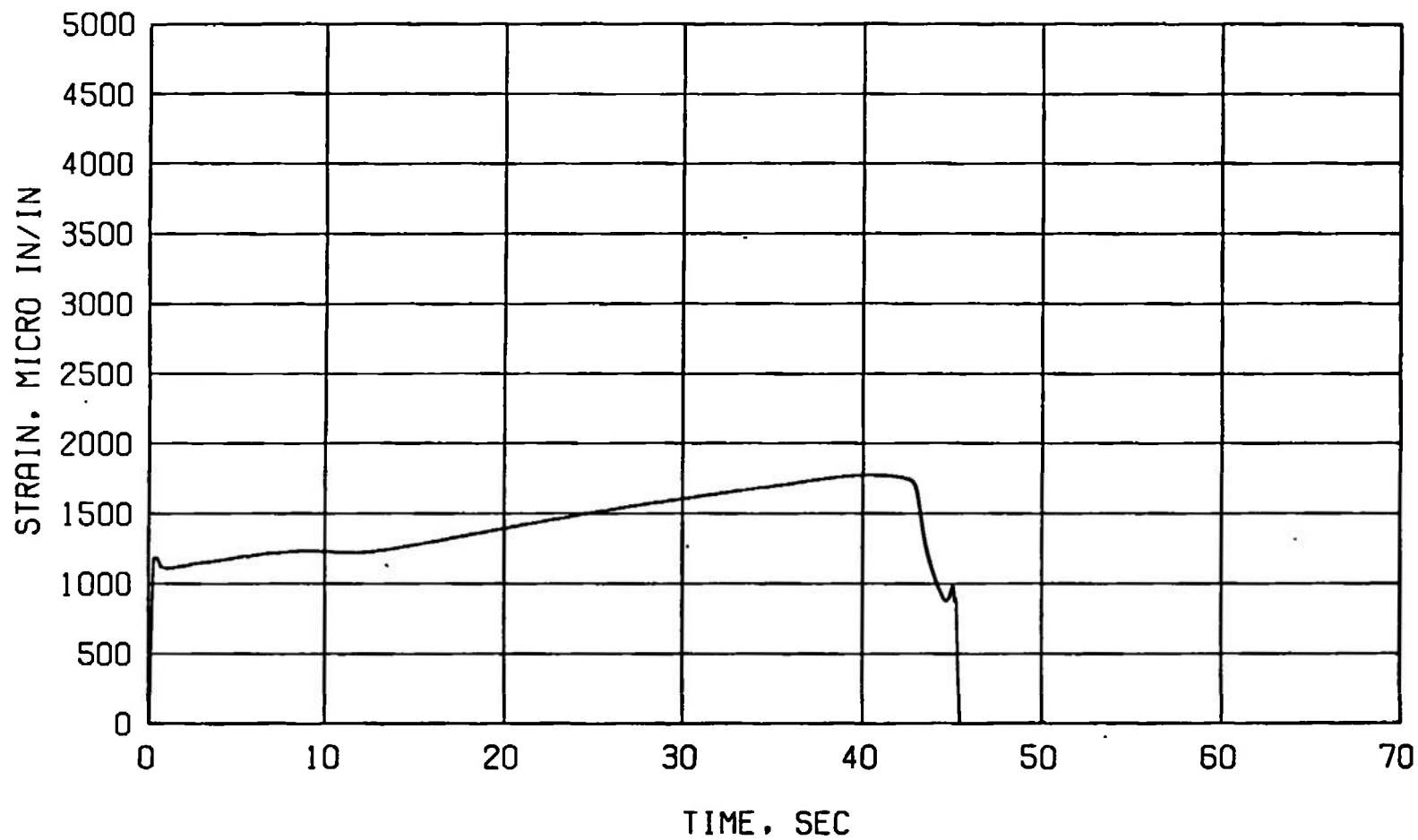


d. Nozzle strain 3D
Figure 11. Continued.

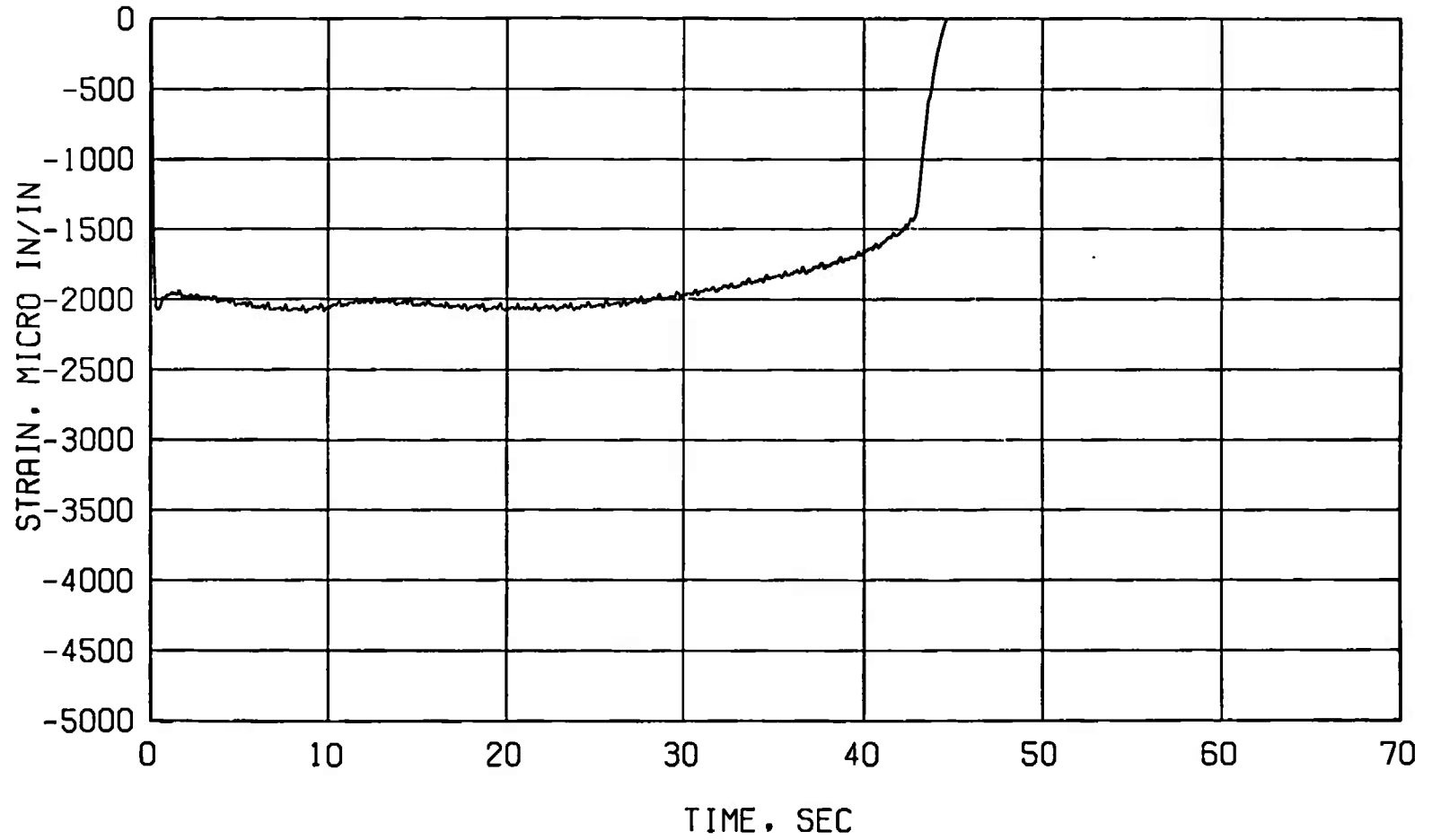


e. Nozzle strain 4A
Figure 11. Continued.

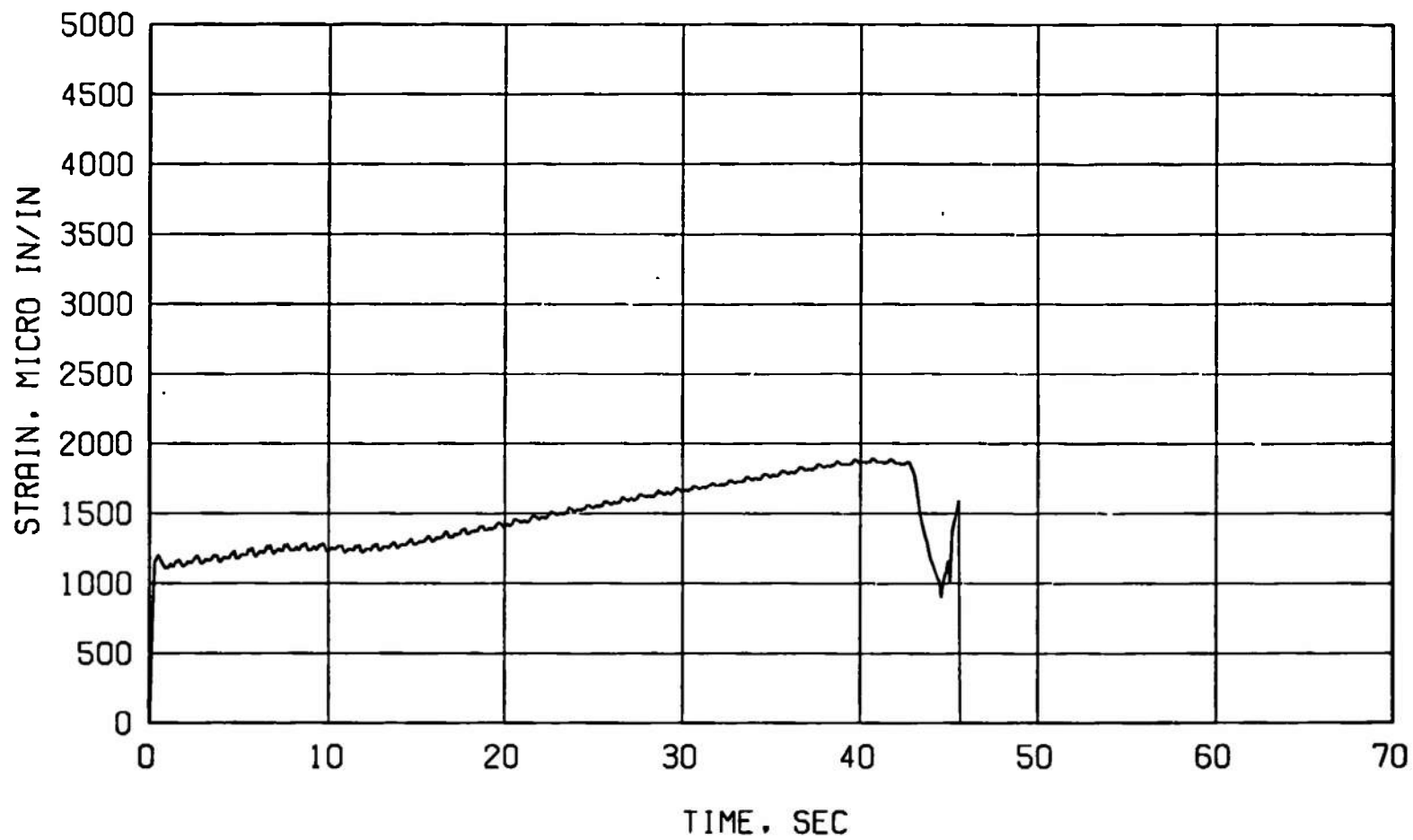
ES



f. Nozzle strain 4B
Figure 11. Continued.



g. Nozzle strain 5A
Figure 11. Continued.



h. Nozzle strain 5B
Figure 11. Concluded.

Table 1. Instrumentation Summary and Measurement Uncertainty

Parameter Designation	STEADY-STATE ESTIMATED MEASUREMENT*								Range	Type of Measuring Device	Type of Recording Device	Method of System Calibration	
	Precision Index (S)			Bias (S)		Uncertainty $\pm(B + t_{95}S)$							
	Percent of Reading	Unit of Measurement	Degree of Freedom	Percent of Reading	Unit of Measurement	Percent of Reading	Unit of Measurement						
Axial Force, lbf	± 0.07	—	147	± 0.06	—	± 0.20	—	10,000 to 14,000 lbf	Bonded Strain-Gage-Type Force Transducers	Sequential Sampling, Millivolt-to-Digital Conversion, and Magnetic Tape Storage Data Acquisition System	In-Place Application of Deadweights Calibrated in the Standards Laboratory		
Total Impulse, lbf-sec	± 0.07	—	147	± 0.07	—	± 0.21	—	—			Resistance Shunt Based on the Standard Laboratory Determination of Transducer Applied Pressure versus Resistance Shunt Equivalence Pressure Relationship		
Motor Chamber Pressure, psia	± 0.40	—	49	± 0.07	—	± 0.87	—	400 to 800 psia			↓	↓	↓
Chamber Pressure Integral, psia-sec	± 0.40	—	49	± 0.07	—	± 0.87	—	—					
Low-Range Chamber Pressure, psia	—	± 0.002 psi	31	—	± 0.006 psi	—	± 0.01 psi (Note 1)	1 to 2 psia					
	± 0.1	—	31	± 0.3	—	± 0.5	—	2 to 10 psia					
	$\pm(0.05\% + 0.005 \text{ psia})$		31	$\pm(0.15\% + 0.015 \text{ psia})$		$\pm(0.25\% + 0.025 \text{ psia})$ (See Note 2)		10 to 50 psia					
Weight, lbm	—	± 0.015 lbm	31	—	± 0.1 lbm	—	± 0.13 lbm	400 to 3,000 lbm	Beam-Balance Scales	Visual Readout	In-Place Application of Deadweights Calibrated in the Standards Laboratory		
Test Cell Pressure, psia	N/A							0.08 to 0.20 psia	Bonded Strain-Gage-Type Pressure Transducer	Sequential Sampling, Millivolt-to-Digital Converter, and Magnetic Tape Storage Data Acquisition System	Resistance Shunt Based on the Standards Laboratory Determination of Transducer Applied Pressure versus Resistance Shunt Equivalence Pressure Relationship		
Test Cell Pressure Integral, psia-sec	N/A							—					

Table 1. Concluded

Parameter Designation	STEADY-STATE ESTIMATED MEASUREMENT*							Range	Type of Measuring Device	Type of Recording Device	Method of System Calibration
	Precision Index (S)			Bias (B)		Uncertainty $\pm(B + t_{95}S)$					
	Percent of Reading	Unit of Measure-meet	Degree of Freedom	Percent of Reading	Unit of Measure-meet	Percent of Reading	Unit of Measure-meet				
Nozzle Temperature, °F	N/A							-200 to 0°F	Copper-Constantan Temperature Transducers	Sequential Sampling, Millivolt-to-Digital Converter, and Magnetic Tape Storage Data Acquisition System ↓	Millivolt Substitution Based on the NBS Temperature versus Millivolt Tables
Nozzle and Case Temperature, °F	—	±0.6°F	31	—	±0.6°F	—	±2.1°F	32 to 360°F	Chromel-Alumel Temperature Transducers		
	—	±0.6°F	31	±0.25	—	±(1.2°F + 0.25% of Reading)		360 to 2,300°F			
Case Strain Indicated (Note 3)	±0.3	—	31	±0.5	—	±1.0	—	400 to 4,000 μ in./in.	Strain Grid		In-Place Application of Resistance Shunt
Vibration, g peak to peak	N/A							10 g peak to peak	Quartz-Type Acceleration Transducer	Charge Amplifiers Onto Magnetic Tape	Voltage Substitution Based on the Standards Laboratory Determination of Transducer Displacement versus Voltage Output Relationship
Time Interval msec	—	±0.25 msec		—	±0.01 msec	—	±0.5 msec	—	Time Pulse Generator	Photographically Recording Galvanometer Oscilloscope	Time Pulse Generator Calibration in the Standards Laboratory
Side Force, lbf	—	±0.14 lbf	6	—	±0.24	—	±0.52	3.5 to 7.5 lbf	Bonded Strain-Gage-Type Force Transducer	Sequential Sampling, Millivolt-to-Digital Converter, and Magnetic Tape Storage Data Acquisition System	In-Place Application of Multiple Force Levels Measured with Force Transducers in the Standards Laboratory

*REFERENCE: CPIA No. 180. "ICRPG Handbook for Estimating the Uncertainty in Measurements Made with Liquid-Propellant Rocket Engine Systems." (AD855130), April 30, 1969.

NOTES:

1. Measurement Made with 15-psia Full-Scale Pressure Transducer
2. Measurement Made with 100-psia Full-Scale Pressure Transducer
3. The Uncertainty of the Case Strain Measurement is Quoted as Indicated Strain. Sources of Error Resulting from the Installation of the Strain-Grid Sensor Which Cannot Be Controlled Are Excluded from the Error Analysis.

Table 2. Summary of TE-M-364-19 Motor Performance

	<u>Specification</u>	
Test Number - R41C-37A	01	Ref. 1
Motor Serial Number	19006	
Test Date	2/4/77	
Average Motor Spin Rate During Firing, rpm	60	
Motor Case Temperature at Ignition, °F	20	
Ignition Delay Time (t_d), sec*	0.004	0.500 Maximum
Ignition Time (t_i), sec**	0.017	
Action Time (t_a), sec***	45.31	
Simulated Altitude at Ignition, ft	122,000	
Maximum Axial Thrust, lbf	13,174	15,000 Maximum
Measured Total Impulse (based on t_a), lbf-sec		
Average of Four Channels of Data	539,890	
Maximum Channel Deviation from Average, percent	0.04	
Chamber Pressure Integral (based on t_a), psia-sec		
Average of Two Channels of Data	26,130	
Maximum Channel Deviation, percent	0.45	
Vacuum Total Impulse (based on t_a), lbf-sec	541,851	
Vacuum Total Impulse (based on t_{op}), lbf-sec	545,152	545,999 \pm 1 %
Vacuum Specific Impulse (based on t_a), lbf-sec/lbm		
Based on the Manufacturer's Stated Propellant Weight	285.12	
Based on Expended Mass (AEDC)	283.35	
Vacuum Specific Impulse (based on t_{op}), lbf-sec/lbm		
Based on the Manufacturer's Stated Propellant Weight	286.86	
Based on Expended Mass (AEDC)	285.07	

*Ignition delay time is the time interval from application of ignition voltage to the time that chamber pressure has risen to 10 percent of maximum ignition pressure.

**Ignition time is the interval from application of ignition voltage to the time that chamber pressure has risen to 90 percent of the maximum chamber pressure reached during the first 500 msec.

***Action time is the interval from the end of ignition time until chamber pressure reaches 100 psia on the descending portion of the pressure-versus-time curve.

****Operation time is the time interval from the first perceptible indication of thrust until the thrust returns to zero.

Table 3. Summary of TE-M-364-19 Motor Physical Dimensions

Test Number - R41C-37A	01
Motor Serial Number	19006 (Q2)
Test Date	2/4/77
Motor Spin Rate, rpm	60
AEDC Prefire Motor Weight, lbm	2423.48
AEDC Postfire Motor Weight, lbm	511.16
AEDC Expended Mass, lbm	1912.32
Manufacturer's Stated Propellant Weight*, lbm	1900.40
Nozzle Throat Area, in. ²	
Prefire	10.915
Postfire	12.044
Change from Prefire Measurement, percent	10.34
Nozzle Exit Area, in. ²	
Prefire	446.791
Postfire	452.158
Change from Prefire Measurement, percent	1.20

*Does not include igniter weight

Table 4. Comparison of Development and Qualification Motor Tests

Motor Serial Number	19001 (D1)	19002 (D2)	19003 (Q1)	19006 (Q2)
Motor Case Temperature at Ignition, °F	27	111	19	20
Ignition Delay Time (t_d), msec*	0.006	0.007	0.003	0.004
Operation Time (t_{op}), sec**	50.00	45.80	52.77	53.93
Simulated Altitude at Ignition, ft	121,000	120,000	121,000	122,000
Maximum Axial Thrust, lbf	12,429	13,863	12,768	13,174
Vacuum Total Impulse (based on t_{op}), lbf-sec	534,992	537,917	535,551	545,152
Vacuum Specific Impulse (based on t_{op} and AEDC expended mass), lbf-sec/lbm ^{OP}	284.79	286.47	285.52	285.07
AEDC Expended Mass, lbm	1878.56	1877.73	1875.70	1912.32
Manufacturer's Stated Propellant Weight, lbm***	1860.00	1860.00	1861.52	1900.40
Nozzle Throat Area, in. ²				
Prefire	10.919	10.904	10.904	10.915
Postfire	11.854	11.876	11.866	12.044
Change from Prefire, percent	8.56	8.91	8.82	10.34
Nozzle Exit Area, in. ²				
Prefire	449.975	446.023	450.056	446.791
Postfire	452.981	450.752	456.168	452.158
Change from Prefire, percent	0.66	1.06	1.36	1.20

*Ignition delay time is the time interval from application of ignition voltage to the time that chamber pressure has risen to 10 percent of maximum ignition pressure.

**Operation time is the time interval from the first perceptible indication of thrust until thrust returns to zero.

***Does not include igniter weight.